Accepted Manuscript

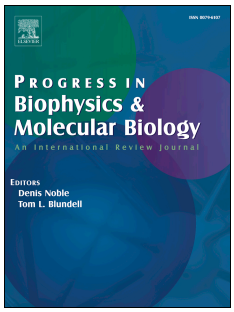

Adding dimension to cellular mechanotransduction: Advances in biomedical engineering of multiaxial cell-stretch systems and their application to cardiovascular biomechanics and mechano-signaling

O. Friedrich, D. Schneidereit, Y.A. Nikolaev, V. Nikolova-Krstevski, S. Schürmann, A. Wirth-Hücking, A.L. Merten, D. Fatkin, B. Martinac

PII: S0079-6107(17)30036-6

DOI: 10.1016/j.pbiomolbio.2017.06.011

Reference: JPBM 1222

To appear in: *Progress in Biophysics and Molecular Biology*

Received Date: 11 February 2017

Revised Date: 8 June 2017

Accepted Date: 19 June 2017

Please cite this article as: Friedrich, O., Schneidereit, D., Nikolaev, Y.A., Nikolova-Krstevski, V., Schürmann, S., Wirth-Hücking, A., Merten, A.L., Fatkin, D., Martinac, B., Adding dimension to cellular mechanotransduction: Advances in biomedical engineering of multiaxial cell-stretch systems and their application to cardiovascular biomechanics and mechano-signaling, *Progress in Biophysics and Molecular Biology* (2017), doi: 10.1016/j.pbiomolbio.2017.06.011.

Adding Dimension to cellular Mechanotransduction:

Advances in Biomedical Engineering of multiaxial Cell-Stretch Systems and their Application to cardiovascular Biomechanics and Mechano-Signaling

O. Friedrich[1,2,3,4], D. Schneidereit[1,3,#], Y.A. Nikolaev[2,5,#], V. Nikolova-Krstevski[2], S. Schürmann[1,3], A. Wirth-Hücking[1], A.L. Merten[1], D. Fatkin[2,6,7], B. Martinac[2,*]*

[1] Institute of Medical Biotechnology, Friedrich-Alexander-University Erlangen-Nürnberg, Paul-Gordan-Str. 3, 91052 Erlangen, Germany

[2] Victor Chang Cardiac Research Institute, Sydney, 2010 NSW, Australia

[3] Erlangen Graduate School in Advanced Optical Technologie (SAOT), Friedrich-Alexander-University Erlangen-Nürnberg, Paul-Gordan-Str. 7, 91052 Erlangen, Germany

[4] Muscle Research Center Erlangen (MURCE), Friedrich-Alexander University Erlangen-Nürnberg

[5] School of Biomedical Sciences and Pharmacy, University of Newcastle, Newcastle, New South Wales 2308, Australia

[6] St Vincent's Clinical School, Faculty of Medicine, University of New South Wales, Darlinghurst, NSW 2010, Australia

[7] Cardiology Department, St Vincent's Hospital, Darlinghurst, NSW 2010, Australia

[#]: these authors contributed equally

[*]: corresponding authors, e-mail:

oliver.friedrich@mbt.uni-erlangen.de, b.martinac@victorchang.edu.au

Running title: 3D mechanotransduction devices for cardiac tissue

Key words: cardiac muscle, mechanotransduction, TRPC channel, Ca^{2+} fluorescence, biomedical engineering, IsoStretcher

Abstract:

Hollow organs (e.g. heart) experience pressure-induced mechanical wall stress sensed by molecular mechano-biosensors, including mechanosensitive ion channels, to translate into intracellular signaling. For direct mechanistic studies, stretch devices to apply defined extensions to cells adhered to elastomeric membranes have stimulated mechanotransduction research. However, most engineered systems only exploit unilateral cellular stretch. In addition, it is often taken for granted that stretch applied by hardware translates 1:1 to the cell membrane. However, the latter crucially depends on the tightness of the cell-substrate junction by focal adhesion complexes and is often not calibrated for. In the heart, (increased) hemodynamic volume/pressure load is associated with (increased) multiaxial wall tension, stretching individual cardiomyocytes in multiple directions. To adequately study cellular models of chronic organ distension on a cellular level, biomedical engineering faces challenges to implement multiaxial cell stretch systems that allow observing cell reactions to stretch during live-cell imaging, and to calibrate for hardware-to-cell membrane stretch translation. Here, we review mechanotransduction, cell stretch technologies from uni- to multiaxial designs in cardio-vascular research, and the importance of the stretch substrate-cell membrane junction. We also present new results using our *IsoStretcher* to demonstrate mechanosensitivity of Piezo1 in HEK293 cells and stretch-induced Ca^{2+} entry in 3D-hydrogel-embedded cardiomyocytes.

1. Introduction

Mechanosensation and mechanotransduction enable tissues and cells to interact with their environment and to respond to mechanical stimuli. Mechanosensing also plays an important role in body homeostasis when the filling volume and pressure of hollow organs need to be monitored and regulated. In the cardiovascular system, blood pressure in vessels is sensed to control cardiac output. Research in the field of prokaryotic mechanosensation has taught us much about the mechanisms at the interface of the protein-lipid bilayer junction. In the cardiovascular system in mammals and humans, the ion channels building up the molecular biosensors are different to prokaryotic ones (Lau et al. 2016, Friedrich et al. 2012), and their expression profiles may correlate with disease states (Randhawa et al. 2015, Song et al. 2014, Mohl et al. 2011), changing stress profiles during development (Heckel et al. 2015) and modulation of electrical coupling in the heart (Thompson et al. 2011, Nishimura et al. 2008). In many case, the molecular identity of stretch-activated ion channels is not yet known, in particular in the domain of mechano-electrical feedback (MEF) in the heart. In other cases, it is still a matter of debate whether ion channel candidates that correlated with pathological stress responses were primarily mechanosensitive or secondarily activated by G-protein coupled receptor (GPCR) mechanosensing units (Hill-Eubanks et al. 2014, Wilson & Dryer 2014, Gottlieb et al. 2008).

Cardiovascular mechanosensing mechanisms have attracted growing interest lately; that includes identification of the respective biosensors as well as their induced signaling cascades. In order to move from correlative studies of ion channel expression under conditions of heart disease to single cell models that allow direct investigation of stretch-induced signals, it is important to reconcile the state of technologies available. Most of our understanding on mechanosensitive channel function and biosensor-actuator loops in cellular systems has either emerged from patch clamp analyses of ionic currents evoked by applying defined negative pressure levels or osmotic stress to the native membrane (Seth et al. 2009), after heterologous expression or reconstitution of ion channels in artificial lipid bilayers or vesicles (Ridone et al. 2015, Shen et al. 2015, Kamaraju et al. 2010, Maroto et al. 2005), or using linear stretch to cells by actuating attached carbon tube rods and performing live-cell imaging (Prosser et al. 2013, 2011).

In this paper, we (i) review evidence from *in vivo* and *in vitro* studies linking physiological and pathological mechanical stress conditions to involvement of mechanosensitive ion channels, their putative molecular identity and mechanosensitivity, and (ii) provide an overview of the state-of-the-art and recent developments in biomedical engineering to provide technologies for improved studies of mechano-signaling in the cardiovascular system. Using a recently introduced *IsoStretcher* technology from our lab, we (iii) also provide new evidence for isotropic-stretch-induced signaling in 3D-embedded cardiomyocytes and additional evidence for mechanosensitivity of Piezo1 channels that might be important to explain endothelial-cardiomyocyte mechano-coupling in the heart.

2. Mechanosensitive channels (MSC) in the cardiovascular system as mechanical biosensors

In heart and vasculature, mechanical stress to tissue walls occurs through contractile activity of smooth muscle or cardiac muscle cells, during passive filling of atria or ventricles, pressure pulse wave propagation, as well as shear stress during blood flow sensed by endothelium (reviewed in Hill-Eubanks et al. 2014, Friedrich et al. 2012).

2.1. MSC families and their general biophysical properties

Since their detection in cardiac and vascular tissue, members of the transient receptor potential (TRP) channels family and very recently Piezo1 channels, have become of major interest in cardiovascular mechanotransduction research. Most of the TRP channels involved in fine-tuning of cardiovascular mechano-response have been centered around the subfamilies of the canonical TRPC, melastatin TRPM and vanilloid TRPV non-selective cationic channels (for reviews refer to Yue et al. 2015, Hill-Eulenbanks et al. 2014, Beech 2013, Dietrich & Gudermann 2011, Yin & Kuebler 2010, Watanabe et al. 2008). Those channels are highly expressed in the plasma membrane of cardiomyocytes (CM), endothelial cells (EC) and vascular smooth muscle cells (VSMC). They are activated by a multitude of stimuli, either mechanical (e.g. pressure, wall tension, and shear stress), chemical (e.g. reactive oxygen species, oxidative stress, phospholipids, arachidonic acid, etc.) or temperature.

Generally, TRP channels form cationic channels with a preferential selectivity for Ca^{2+} ions. For instance, TRPV5/6 are highly Ca^{2+} selective ($P_{Ca}/P_{Na} > 100$), TRPM4/5 merely Ca^{2+} selective ($P_{Ca}/P_{Na} < 0.05$), while for the remainder, P_{Ca}/P_{Na} is usually <10 (Yue et al. 2015, Harteneck 2005, Hofmann et al. 2003). Some of the TRP channel subfamilies form homo- or heteromeric tetramer channels, e.g. TRPC1 with TRPC4/5 (Strubing et al. 2001) or TRPC3/6/7 with each other (Hofmann et al. 2002), to name a few combinations (Yue et al. 2015). Several TRP members respond to mechanical stretch. Among canonical TRPC, TRPC1 and TRPC6 were first identified as responding to hydrostatic or osmotic pressure-induced membrane stretch (Spassova et al. 2006, Maroto et al. 2005), although overexpression of TRPC1/6 in heterologous expression systems could not detect any significant increase in mechanosensitive currents, puzzling the translation from single channel data towards ensemble data (Gottlieb et al. 2008). TRPC3 was for a long time not recognized as mechanosensitive on its own, as it usually forms heterotetramers with TRPC6 thus, strongly influencing TRPC6 mechanosensitivity (Quick et al. 2012). As in TRPC6 activation, TRPC3 is likewise activated by GPCR G_q protein kinase C/phospholipase C signaling through the intermediate diacylglycerol (DAG) (Hofmann et al. 1999). However, TRPC3 mechanoactivation (heterologously expressed in CHO-K1 cells exposed to hypoosmotic shock) was shown to induce a clear whole-cell current response that was not influenced by co-expression of a mechanosensitivity-abrogated TRPC6-N143S mutant (Wilson & Dryer 2014). TRPC5 was activated by osmotic challenge and membrane suction, and single channel currents were recorded upon mechanical activation (Shen et al. 2015, Gomis et al. 2008). Several lines of evidence have been presented for TRPC6 mechanosensitivity in heterologous expression systems (Wilson & Dryer 2014, Inoue et al. 2009, Spassova et al. 2006), or in native cells (Anderson et al. 2013, Quick et al. 2012). In mouse CM, immediate activation of non-selective ion currents was noted when the cell membrane was impinged with a glass rod (Dyachenko et al. 2009). The mechanosensitive current component was blocked by GsMTx-4, a hitherto well established highly specific blocker of MSCs (Bowman et al. 2007). GsMTx-4, a 4 kDa peptide isolated from *tarantula stomata* and recombinant available by now, specifically acts on MSC subtypes which may also include members of the TRP family (Gottlieb et al. 2007). Linking cardiomyocyte MSC data to TRPC6 was more

evidently established by use of a pore-blocking TRPC6-antibody able to block both the mechano-activated and the OAG-activated (a DAG analogue) currents in mouse CM, establishing the *in situ* mechanosensitivity of TRP6 (Dyachenko et al. 2009). In HEK and CHO cells heterologously expressing TRPC6, mechanical activation of TRPC6 secondary to GPCR stimulation persisted in the presence of GsMTx4 (Inoue et al. 2009, Spassova et al. 2006), indicating that mechanical and chemical lipid signaling share a common molecular mechanism involving lateral lipid-tension (Spassova et al. 2006). However, similar experiments involving pore-blocking anti-TRPC6 are still missing. Interestingly, in addition to stretch-activation, TRPC6 also seems to contribute to receptor-operated Ca^{2+} mobilizations that are likely to be involved in vasoconstrictor and myogenic responses and pulmonary arterial proliferation (Inoue et al. 2006). Also, TRPC6 seems to play an important regulatory function through receptor-operated Ca^{2+} entry, e.g. involving ß-adrenergic signaling in CM involving snapin (Mohl et al. 2011) **(Fig. 1)**, or hypoxia-induced signaling in pulmonary smooth muscle cells (Tang et al. 2010). Of the TRPV family, TRPV2/4/5/6 have been documented as mechanosensitive, e.g. TRPV2 in murine aorta myocytes (Muraki et al. 2003); TRPV4 in heart valves during development (Heckel et al. 2015), in rat endocardium contributing to atrial volume sensing (Shenton & Pyner 2014), in ventricular CM (Hu et al. 2009) or in cardiac fibroblasts (Adapala et al. 2013); TRPV5/6 in transfected HEK cells (Cha et al. 2013). Of the TRPM family, TRPM3/4/7 seem mechanosensitive (e.g. Li et al. 2014, Numata et al. 2007, Earley et al. 2004).

The multi-transmembrane domain protein channel Piezo1, has recently been identified as inherently mechanosensitive (Syeda et al. 2016). It acts as a membrane biosensor for frictional force in the cardiovascular system (Li et al. 2014a). Piezo1 responds to lateral membrane tension (Cox et al. 2016, Lewis & Grandl 2015, Coste et al. 2012) and is modulated, e.g., by phosphoinositide (Borbiro et a. 2015) and cytoskeletal components (Retailleau et al. 2015, Gottlieb et al. 2012). Using their approach of Piezo1 incorporated into droplet lipid bilayers, Syeda et al. (2016) showed that Piezo1 mechanosensitivity followed the ‘force-from-lipids’ paradigm of a pure lipid-embedded force biosensor responding to mechanical forces within the bilayer without the need for any other cellular components (Teng et al. 2015, Martinac et al. 1990).

2.2. Mechano-signaling in the vasculature

2.2.1. Vascular involvement of TRP channels

A variety of TRP channel members act as NO sensors in the endothelium of the vasculature, being activated by GPCRSs with DAG production and subsequent Ca^{2+} influx. The latter then drives NO production via NO synthases (Yoshida et al. 2006) **(Fig. 1)**. NO diffusing into adjacent smooth muscle cells drives cGMP (cyclic guanosine monophosphate) formation to stimulate myosin light chain phosphatase. This results in relaxation and vasodilation (Nakamura et al. 2007). This mode of vasodilation more or less applies to TRPC1/3/4/5/6 and TRPV1/3/4 through Ca^{2+} entry (Zhang & Guttermann 2012). In VSMC, TRP channels are mainly involved in direct regulation of myogenic tone, either by GPCRs or as part of the autoregulation **(Fig. 1)**. MSC-induced vasoconstriction has been demonstrated for instance for TRPC6 through α1-adrenoceptor-induced, TRPC6-mediated Ca^{2+} entry (Inoue et al. 2001) **(Fig. 1)**. Although the myogenic response (i.e. the increase in smooth muscle tone in response to increased intraluminal pressure to increase vascular resistance and limit flow) primarily depends on L-type Ca^{2+} channel activation, TRP channels modulate this response, e.g. TRPC1/5/6, TRPV1/2/4, TRPM7/8, and maybe more (Yue et al. 2015). In particular, TRPM4 seems to be crucial for cerebral flow autoregulation (Reading & Brayden 2007). In rat posterior cerebral artery smooth muscle cells devoid of endothelium, TRPM4 potentiates the activity of mechanosensitive ENaC (epithelial Na^+ channels) through a putative direct interaction, which probably complements stretch-induced depolarization through ENaC by TRPM4-induced Ca^{2+} entry (Kim et al. 2013) **(Fig. 1)**. This mode did not apply to TRPC6 (Kim et al. 2013), for which direct and GPCR, second messenger-induced activation modes probably apply more exclusively (Inoue et al. 2009). TRPC5 has recently been found to play an essential role as key pressure transducer in systemic blood pressure regulation within the aortic baroreceptors, because $TRPC5^{-/-}$ mice displayed severe daily pressure fluctuations (Lau et al. 2016). For TRPV4, an additional mechanism of activation was shown to result in Ca^{2+} sparklets, subsequently activating BK_{Ca} channels for hyperpolarization and direct muscle relaxation (Sullivan & Earley 2013) **(Fig. 1)**. Interestingly, a VSMC hyperpolarization was also seen when TRPV4 channels were activated in the adjacent EC. This is because of direct electrical coupling through gap junctions in the myoendothelial

complex (Sonkusare et al. 2012) **(Fig. 1)**. Apart from immediate signaling resulting in myogenic control, vascular TRP channels also regulate VSMC proliferation and vascular permeability (Hill-Eubanks et al. 2014). Regarding the most common vascular pathology, hypertension, TRPC3/6 channels are involved in essential hypertension models and rearrange their assembly proportions towards a higher TRPC3 contribution, thus favoring VSMC depolarization (Alvarez-Miguel et al. 2017). Besides regulating flow-induced arteriogenesis, TRPV1/4 channels are also implicated in pulmonary hypertension and hypoxic preconditioning (Parpaite et al. 2016, Randhawa & Jaggi 2015). Ablation of TRPV4 was able to delay and markedly attenuate pulmonary hypertension using siRNA silencing in rats (Yang et al. 2012).

2.2.2. Vascular involvement of Piezo channels

The mechano-biosensor Piezo1 is also expressed in vascular EC and VSMC (Retailleau et al. 2015, Ranade et al. 2014). In fact, Piezo1 was found to be essential for vascular development, as mice deficient for Piezo1 die at mid-gestation with defects in vascular remodeling, possibly due to abrogated flow-induced mechano-signaling (Ranade et al. 2014). The endothelial Piezo1 component of shear-stress-evoked Ca^{2+} influx was assessed as a pivotal vascular mechano-integrator (Li et al. 2014a) that was required for flow-induced endothelial ATP release and subsequent G_q/G_{11}-coupled purinergic P2Y2 receptor stimulation. This in turn results in AKT (protein kinase B) phosphorylation and NOS production with subsequent vasodilation (Wang et al. 2016a) **(Fig. 1)**. In VSMC, the role of Piezo1 has not been extensively reported yet. However, it seems important in hypertension-dependent structural remodeling of small arteries, with a trophic effect in resistance vessels where a Piezo1-induced increase in cytosolic Ca^{2+} stimulated transglutaminases to facilitate protein crosslinking during the remodeling phase in hypertension (Retailleau et al. 2015).

2.3. Mechano-signaling in the heart

2.3.1. Cardiac involvement of TRP channels

In early studies, a non-selective Ca^{2+}-activated cation channel sharing similarities with TRPM4 and TRPM5 was described in human atrial CM to be involved in after-depolarizations and arrhythmias during cardiac Ca^{2+} overload (Guinamard et al. 2004). Later, TRPC1 was found to be upregulated in mouse hearts with a congenital

cardiac hypertrophy phenotype related to a dominant-negative form of the transcription repressor neuron-restrictive silencer factor (NRSF). In this model, TRPC1 transfection into primary CM increased NFAT (nuclear factor of activated T-cells) activity, thus stimulating cardiac hypertrophy genes (Ohba et al. 2007, 2006) **(Fig. 1)**.

Canonical TRP channels have been robustly described to be crucially involved in development of cardiac hypertrophy under pathophysiological conditions (Seth et al. 2009, Kuwahara et al. 2006, Nakayama et al. 2006, Onohara et al. 2006). TRPC1$^{-/-}$ mice are functionally protected from cardiac hypertrophy in pressure-overload models and preserve cardiac function when subjected to hemodynamic and neuro-hormonal stress (Seth et al. 2009). TRPC1/3/6 were upregulated in pressure-overload and calcineurin-mediated cardiomyopathy (Kuwahara et al. 2006, Nakayama et al. 2006). *In vivo* studies in transgenic TRPC3-overexpressing mice document increased hypertrophy when challenged with angiotensin-II or phenylephrine through TRPC3-mediated, Ca^{2+}-dependent calcineurin/NFAT activation (Nakayama et al. 2006). In TRPC6 overexpressing models, hypertrophy signaling is already activated without neuro-hormonal stimuli (Kuwahara et al. 2006). More specifically, heteromeric complexes of TRPC1/4/5 and TRPC3/6/7 have been suggested to mediate the pathological hypertrophy responses (Eder & Molkentin 2011, Wu et al. 2010). The reason why some TRPC isoforms may be more severely involved in calcineurin signaling over others (e.g. TRPC6 over TRPC3) even without GPCR involvement may be their differential intrinsic mechanosensitivity. As a consequence of aberrant calcineurin/NFAT signaling, TRPC1/3/6 genes containing conserved NFAT consensus sites become upregulated. This sustains a vicious remodeling cycle.

Generally, calcineurin signaling is thought to be exclusively associated with pathological cardiac hypertrophy signaling (Heineke & Ritter 2012). In fact, it was found unaltered during physiological cardiac hypertrophy in swim-trained rats (Yeves et al. 2014). Thus, a role of TRPC channels to a hitherto regulating function in normal growth signaling in CM is still elusive. In this regard, it is interesting to note that on a beat-to-beat basis in isolated murine CM subjected to external field stimulation, we could detect a mechanosensitive component to systolic intracellular Ca^{2+} that accounted for ~5 % of systolic Ca^{2+} amplitude and was blocked by GsMTx-4

(Friedrich et al. 2012). Although the identity of the underlying MSC has not yet been elucidated, this may point towards an interesting direct involvement of TRP channels to regulating intracellular Ca^{2+} and contractility during normal beating. Store-operated Ca^{2+} entry has been associated with TRPC channels in rat neonatal ventricular CM to be activated by a G-protein coupled Ca^{2+} sensing receptor (CaR) to enhance apoptosis (Sun et al. 2010). This was subsequently extended towards adult rat CM showing that also TRPC3 but not TRPC1 was upregulated by CaR-induced TRPC-activated Ca^{2+} entry (Feng et al. 2011). TRPC3 overexpression in turn increases CM sensitivity to Ca^{2+} overload, driving affected CM into apoptosis instead of necrosis (Shan et al. 2008). Apart from being involved mostly in pathophysiological cardiac processes (hypertrophy, arrhythmia, Bode et al. 2001), we have found TRPC6 being also involved in receptor-operated Ca^{2+} entry, where it modulates cardiac contractility via α_{1A}-mediated signaling in an enhanced cardiac α_{1A}-receptor (α_{1A}-R) expressing mouse model but also, to a lesser extent, in wt-littermates. This α_{1A}-R effect of TRPC6 channel Ca^{2+} entry was abrogated by TRPC6 pore-blocking antibody and thus, shows the importance of TRPC6 for cardiac contractility already under physiological α_{1A}-R signaling (Mohl et al. 2011). Apart from this, not much information on the *physiological* role of TRPC in CM is available.

For TRPM, TRPM4 is functionally expressed in sino-atrial cells and a key player for heart rhythm generation and maintenance (Demion et al. 2007), as well as for conduction along the Purkinje fibres (Hof et al. 2016). TRPM4 also seems to negatively regulate on angiotensin II-induced, TRPC-mediated cardiac hypertrophy (Kecskes et al. 2015); TRPM7 is essential for correct cardiac embryonic development (Sah et al. 2013) and regulates HCN4 expression to modulate diastolic membrane depolarization and automaticity in the sino-atrial node (Sah et al. 2013a). TRPM2 was shown to act as a double-edged sword. In some studies, it seemed essential to maintain CM bioenergetics (i.e. TRPM2-mediated Ca^{2+} influx maintains mitochondrial function following hypoxia-reoxygenation by reducing mitochondrial oxidants, Hoffman et al. 2015), while in other studies, its activation resulted in mitochondrial membrane disruption, cytochrome c release, caspase-3-dependent chromatin fragmentation and myocyte death (i.e. following ischemia-reperfusion injury, Yang et al. 2006) **(Fig. 1)**.

TRPV functionality in CM is very scarcely documented in the literature. In a very interesting study, TRPV2 has been recently shown to mediate mechanical forces necessary to maintain coupling between neighboring CM at the level of intercalated discs. Within four days of eliminating TRPV2 from hearts of adult mice, cardiac function declined severely, with vast structural disorganization of intercalated disc areas (Katanosaka et al. 2014). A few days later, CM biomechanics and Ca^{2+} handling were markedly impaired, and anabolic IGF-1/PI3K/AKT signaling was downregulated (Katanosaka et al. 2014). This may provide a first link between a member of the TRP family and protein synthesis pathways that might be involved in physiological cardiac growth and hypertrophy rather than the link to pathological hypertrophy through calcineurin/NFAT signaling by TRPC members **(Fig. 1)**. TRPV4 also forms a mechanosensitive Ca^{2+} channel in rat ventricular CM (Hu et al. 2009). TRPV4 channels have been more detailed investigated in cardiac fibroblasts where they are important in TGF-ß1 (transforming growth factor)-induced differentiation to myofibroblasts (Adapala et al. 2013, Thodeti et al. 2013). Very novel data from our own research indicates that TRP channels, i.e. TRPC6, are also important to deliver mechanically-induced soluble crosstalk between different cardiac cell types. Specifically, atrial EC that were cyclically subjected to uniaxial elastomer stretch (methodologies **see 3.7.**) released soluble factors that induced Ca^{2+} entry into induced pluripotent stem (iPS) cell-derived CM through a TRPC6-dependent mechanism (Nikolova-Krstevski et al. 2017), thus opening new venues for mechano-signaling across cell-type borders in the heart.

2.3.2. Cardiac involvement of Piezo channels

For Piezo1, there is no published study yet available tackling its mechanistic role to intrinsic cardiac function or involvement in cardiac pathology. A recent study correlated increased mechanosensitive micro-RNA 103a expression in acute myocardial infarction patients with inhibited Piezo1 channel expression however, the mechanistic implications are still elusive (Huang et al. 2016).

Fig. 1 envisions the role of mechanosensitive channels and their respective molecular identity to cardiac and vascular function.

3. Technologies to apply cell- and membrane stretch and to assess mechanotransduction pathways

Life science research dedicated to study mechanotransduction in cellular systems requires technologies that transduce external forces (e.g. indentation, shear-forces or pressure) to the membrane of cells. Such methodologies have developed from using the same devices to assess channel readouts, i.e. microelectrode-based electrophysiology techniques, to sophisticated elastomer-based actuators. In most latter cases, optical readouts have been implemented, in particular fluorescence microscopy. The following sections will provide details of the different methodologies developed over the last two decades, their strengths and weaknesses and potential fields of applications to study mechanotransduction. A focus will be on recent developments of elastomer-based systems to apply 2D (and even 3D) uniaxial or multiaxial and isotropic stretch systems and their distinct differences to point-to-point stretch systems, in particular when applied to cells of the cardiovascular system. A particular emphasis is on the requirement to calibrate 'hardware stretch' of elastomer substrates to 'membrane stretch' of the cell membrane which strongly depends on coating protocols involved, the tightness of the elastomer-cell junction and the type of cells involved. In principle, this has to be assessed for each cell type and technology applied. In the following sections, the different approaches to local and global cellular stretch alongside with clarification of directionality nomenclature are presented.

3.1 Pipette-suction electrophysiology to study mechano-signaling (Fig. 2A)

A very classical setting to investigate mechanosensitive membrane channels derives from the patch clamp technique (Hamill et al. 1981, Neher & Sakman 1976). A tip of a small pipette pulled from glass capillaries heated with platinum filaments and filled with saline is approached towards a cell membrane to establish an electrical 'seal' upon close contact with the membrane. A patch of membrane containing single or ensembles of ion channels becomes accessible to voltage pulses and ion current recordings (Neher et al. 1978). The trick in establishing giga-ohm seals as a requirement to record pA-currents through individual channels is the application of negative pressure pulses to the membrane in order to tighten the glass-membrane junction and to obtain a cell-attached patch of small diameter (~1-3 µm). In early studies on isolated inside-out patches from neonatal rat CM membranes, application

of -10 mmHg pressure to the membrane evoked robust inward cationic single channel currents (single channel conductance ~40 pS) that were blocked by 1 µM Gd^{3+}, an unspecific blocker of MSC (Sadoshima et al. 1992, **Fig.2A**). In another study in rat aorta EC, positive pressure applied to the membrane reversibly increased open probability of MSC (slope conductance for inward currents ~6 pS, ionic permeability P_{Ca}:P_{Na}:P_K of 3.5 : 1 : 1.4) (Marchenko & Sage 1997). 100 µM of Gd^{3+} or La^{3+} blocked these currents. Although suction and positive-pressure applications via patch pipettes represent an elegant measure to combine mechanical membrane actuation with direct recordings from membrane ion channel biosensors, limitations are given by the fact that electro-neutral ion movements through MSC may go completely undetected. More severely, pressure-induced cationic currents in patch clamp usually are only restricted to acute stimulus-biosensor recordings restricted to the membrane level, i.e. they cannot capture intracellular signaling events. Also, this technique only captures local mechanical stress to the membrane and local sub-membrane cytoskeletal elements. Applying suction to the membrane modifies the stress distribution in response to force application, which is in particular important if recordings are performed in the excised patch configuration given that there is a significant difference between the stress developed in the outer and in the monolayer of the membrane bilayer (Bavi et al. 2014). Finally, throughput of pipette-based mechanotransduction studies in patch-clamp configuration is rather limited, and no robust high-throughput solutions exist.

3.2. Hypoosmotic cell swelling to study mechano-signaling (Fig. 2B)

Mechanotransduction response to osmotic challenge, in particular hypoosmotic stress, is a rather archaic reaction of cells to changes in environmental osmolarity (Kloda & Martinac 2002). Upon decrease in extracellular osmolarity, water moves from extra- to intracellular in order to balance the osmotic gradient. The conduit for these water movements is through membrane aquaporin channels which are also expressed in CM (Rutkowskiy et al. 2013a), cardiac and vascular EC and fibroblasts (Rutkowskiy et al. 2013, 2013a). The resulting cell swelling activates mostly Cl^--channels in order to reduce the cell's salt content to counteract swelling. The most common readouts to monitor changes during hypotonicity-induced swelling are electrophysiology or fluorescence microscopy techniques. In canine CM subjected to

hypoosmotic swelling, whole-cell recordings from perforated patches revealed strong activation of inward-rectifying, swelling-activated currents that reversed near -60 mV, and were inhibited by 10 µM Gd^{3+}, which also reduced cell swelling (Clemo et al. 1998) **(Fig. 2B)**. This swelling-activated inward current remained persistently activated in CM from dogs with congestive heart failure (Clemo et al. 1998). Swelling-activated Cl^--currents ($I_{Cl,swell}$) are more frequent in atrial over ventricular CM (Vandenburg et al. 1994), and have been associated with arrhythmogenesis, myocardial injury, preconditioning, apoptosis and mechano-electrical feedback (Baumgarten & Clemo 2003).

While hypoosmotic swelling can be regarded as a useful tool to study global mechanotransduction in cells in general, it has to be considered with caution when applied to cardiac cells, in particular CM. While in small and more rounded cells osmotic swelling can be considered as an isotropic stretch, it may not so in CM, where the highly organized cytoskeleton apparatus and the presence of both surface and tubular membrane systems result in unequal lateral and axial stiffness (for skeletal muscle, see Higuchi 1987). For example, hypoosmotic stress has been shown to cause sealing of t-tubules, impeding cardiac ec-coupling (Moench et al. 2013), or to recruit caveolae as membrane reserves to the sarcolemma to limit mechanosensitive $I_{Cl,swell}$ activation in CM (Kozera et al. 2009). Moreover, osmotic swelling in CM induces loss of glutathione and increases the sensitivity towards oxidative stress (Lee et al. 2009). This sustains a vicious cycle to drive CM dysfunction as a consequence of osmotic swelling in pathological conditions of cell hypoxia with consequent ATP depletion and Na^+ overload through Na^+/K^+-ATPase failure (Takeuchi et al. 2006), e.g. during ischemia/reperfusion. Thus, hypoosmotic swelling may reflect a global membrane stretch model mimicking pathophysiological hypoxia-associated cellular CM edema and dysfunction rather than a physiological stimulus to study mechanotransduction. It is interesting to note that a very recent study was able to demonstrate a cardio-protective effect for the tarantula peptide GsMTx-4 in ameliorating ischemia and reperfusion-induced CM swelling and dysfunction (Wang et al. 2016).

3.3. Shear-flow to study mechanotransduction (Fig. 2C)

Blood flow in the cardiovascular system induces shear-stress that predominantly affects mechanotransduction in the contact cell layers, i.e. the endothelium. The effects of shear stress on endothelial function, in particular on the NOS, are well presented in Balligand et al. (2009). That review also nicely provides an integrated view of endothelial-cardiomyocyte cross-talk by physical forces. The influence of flow-induced shear stress on endothelial ROS production, epigenetics, autophagy, inflammation, focal adhesion complex homeostasis and endothelial-smooth muscle cell cross-talk is well presented in a recent review by Christiakov et al. (2017).

Early designs of systems to apply laminar flow to cell cultures go back to the early 80s (Krueger et al. 1971) and since then, a multitude of fluidics, micro-fluidics, lab-on-a-chip systems and bioreactor-based systems have been employed, both commercially and on a research-lab scale (Davis et al. 2015). For details on advances in biomedical engineering of flow- and combined physical forces technologies in the cardiovascular system, the interested reader is referred to the very elegant review by Davis et al. (2015). Here, only a few very recent developments shall be mentioned.

An important reaction of EC towards shear-stress in flow-cell environments is their repatterning and polarization towards the flow direction (Morgan et al. 2012, Levesque & Nerem 1985). In order to provide a miniaturized system to study EC mechanotransduction using high-resolution fluorescence microscopy, a recently introduced microfluidics system allowed to monitor Ca^{2+} reactions to variations in global and local shear stresses using advanced UV protein micro-patterning through chromium synthetic quartz photomask for control of EC elongation and orientation (Lafaurie-Janvore et al. 2016). The flow field in this system was controlled by coupling the micro-patterned substrate to the microfluidics chamber to fit on a microscope stage. Using this system, (i) lamellipodia formation could be resolved online in the downstream portion, and retraction in the upstream portion of EC, and (ii) intracellular Ca^{2+} waves with propagation direction determined by cell polarization rather than flow direction were demonstrated. Varying the adhesive micro-patterning grating distance, EC shape could be controlled at both the monolayer and the single cell level (Lafaurie-Janvore et al. 2016).

Older microfluidics systems containing one laminar flow channel usually lacked the throughput aspect in a sense that 'shear-stress level – response' studies had to be conducted in different experimental assays exposing cells to either high- or low shear stress regimes. Multi-shear design has been introduced as a solution where a series of parallel channels with varying diameters, respective different flow resistances, were connected to a single inlet-outlet (Gutierrez et al. 2008). A major downside to such systems can be seen in the separate handling of the no-flow control group requiring a separate device as well as in the lack of interaction from EC residing at different shear-stress areas, which would map more closely the situation *in vivo* with highly non-linear temporal and spatial flow profiles. To overcome these constraints, a diamond-shaped microfluidics shear device was engineered hosting high- and low-shear zones within the same chamber under identical culture conditions (Zhang et al. 2014). Parallel arrangement of compartments allowed generation of shear stresses of varied magnitudes to which cells were simultaneously exposed (Zhang et al. 2014). A cheap and biocompatible microfluidics device was built and introduced by another group using fluidics circuits engraved in polydimethyl-siloxane (PDMS) elastomers and sealed to a glass surface onto which cells are grown (Fede et al. 2014). By modulating the time of atomic oxygen and ozone atmosphere exposure required to generate silanol groups by oxidation of the methyl groups to increase hydrophilicity of the elastomer, a tight microfluidics device that withstands high pressure flows, yet providing a reversible seal between two surfaces, was produced. With this system, human umbilical vein endothelial cells (HUVEC) were successfully cultured under various flow conditions, and maximum detachment flows (50 µl/min) were assessed (Fede et al. 2014). In order to approach ways to increase throughput in microfluidics circulation devices, Satoh et al. (2016) developed a system containing three independent circulation culture units in which HUVEC cells could be cultured under physiological shear stresses using a pneumatic pressure system. Even further on the path to increasing throughput was presented by a novel, low-cost multi-functional fluid flow device that can be scaled up to be used to provide flow-induced shear stress to cells cultured in 96 well plate format (Lyons et al. 2016).

3.4. Physical membrane indentation to study mechanotransduction (Fig. 2D)

Indentation of cell membrane uses point or plane impression by gently pushing blunt processes or styluses towards the cell membrane under micromanipulator guidance. Early approaches elegantly used a reverse operation of atomic force microscope levers arms to act as a micro-indenter (Charras & Horton 2002). However, only few studies exist applying this to cells of the cardiovascular system to study mechano-signaling, e.g. in cardiac fibroblasts (Codan et al. 2014). More commonly, mechanical point indentation is performed using fire-polished large diameter (~2-4 µm tip) glass pipettes to locally indent the membrane to different depths while, for instance, recording whole cell currents in the same session with an opposed patch pipette (Huang et al. 2013), or using two-electrode voltage clamp (Saitou et al. 2000). In isolated cardiac fibroblasts mechanically deformed by patch pipettes that allowed both indentation as well as local stretch, compression resulted in membrane depolarization through a mechanosensitive non-selective cation conductance while stretch hyperpolarized the fibroblast (Kamkin et al. 2003). Subsequently, a model was put forward to explain mechanical coupling between cardiac fibroblasts and CM where the former can function as mechano-electrical transducers possibly involved in mechano-electrical feedback (Kamkin et al. 2005).

In a study using a cell-attached glass stylus to shear the upper cell part versus the substrate-attached bottom of mouse ventricular CM, deformation activated a nearly voltage-independent GsMTx-4 sensitive non-selective cation conductance that was inhibited by anti-TRPC6 antibody (Dyachenko et al. 2009). Another study used a heavily fire-polished glass capillary as a mechanical probe, sinusoidally driven either in the plane of the membrane or normal to the membrane of isolated rat ventricular myocytes in conjunction with voltage-clamp to record mechanosensitive currents that had two components: a brief large inward spike, followed by a more sustained smaller cationic inward current (Bett & Sachs 2000) that was comparable in amplitude to that from cells undergoing axial strain (see below, Zeng et al. 2000). It was speculated that the initial sharp inward current reflects a collapse or relaxation of cytoplasmic elements exposing mechanosensitive sensors to stress (Bett & Sachs 2000).

As with micro-indentation, indenters are individually actuated towards a single cell at a time, experimental throughput is rather limited and high-throughput systems are not available.

3.5. Magnetic tweezer local membrane pinch to study membrane complex biomechanics (Fig. 2E)

Magnetic tweezers or magnetic bead micro-rheometers were originally designed to allow generation of forces up to 10 nN transmitted between cell membranes and paramagnetic beads using a magnetic coil-induced field (Bausch et al. 1998, Ziemann et al. 1994). Magnetic beads of ~5 µm size are attached to the plasma membrane after coating with extracellular matrix proteins, e.g. fibronectin, to target binding to integrin receptors for focal adhesion complex (FAC) anchorage. Following attachment, a magnetic field is established via the magnetic coils, and the membrane-bead complex is pinched towards the coil. Using this approach, local visco-elastic moduli of the cell envelope and the adjacent cytoplasm components can be assessed (Bausch et al. 1998). This technique can only detect local lateral visco-elasticity of a complex containing membrane, focal adhesions and cytoskeletal elements to unknown extents. In addition, results strongly depend on the tightness of the bead-fibronectin-integrin interaction. Thus, the magnetic tweezer-derived biomechanics parameters do not represent a single element but the summed contribution of those elements directed perpendicular to the cell membrane. Therefore, the strength of this technique is to assess lateral stiffness of the pan-membrane complex, for instance in cellular model systems deficient of focal adhesion molecules (Alenghat et al. 2000). Magnetic tweezer technologies have mostly been applied to fibroblasts (Alenghat et al. 2000) and cancer cells (Swaminathan et al. 2011). In EC, cyclic local forces applied to FAC were found to recruit actin filaments towards the FAC area (Ueki et al. 2010). When co-cultured with invasive tumor cells, magnetic tweezer approaches revealed tumor cells to alter the mechanical properties of ECs by reducing their lateral stiffness (Mierke 2011). Due to the local nature of the technology to only assess lateral membrane-FAC visco-elasticity and not axial biomechanics, magnetic tweezers cannot be used to axially stretch CM (referring to their longitudinal axis). There seems to be no study available where CM have been subjected to magnetic tweezer experiments.

Due to coil geometries and the induced magnetic fields, miniaturization and parallelization of multiple tweezers to increase the throughput of such experiments has not been documented in the literature yet.

3.6. Axial global cellular stretch via traction rods to study mechanotransduction (Fig. 3)

The rod-shaped geometry of CM assigns two major axes, a longitudinal axial and a short lateral axis. Both define differing axial and lateral visco-elastic elements due cytoskeletal arrangement (Higuchi 1987). Unlike axial stretch in skeletal muscle fibres, which is easily implemented in force transducer and actuation systems due to their long lengths, manually attaching CM (~100-150 µm length) to mechanical actuation systems is not straightforward. One of the first studies to apply axial stretch to single isolated CM employed impalement of myocytes with glass microelectrodes near both ends and applying small stretches before chemical Ca^{2+} activation (Fabiato & Fabiato 1975). In the setting of this section 3.6., 'axial stretch' refers to the long axis of the mechanically clamped CM and involves a uniaxial stretch (to be in line with the nomenclature with 3.7., see below).

Moving towards intact and electrically excitable preparations, single-barreled pipettes with vacuum suction were introduced to mechanically attach rat CM, and to record forces during electrical stimulation (Brady et al. 1979). In an elaborate approach to combine whole-cell electrophysiology with axial pipette-stretch to single CM, Sasaki et al. (1992) fabricated heat-polished glass pipettes with a ball-shaped plunger lowered to the CM membrane to restrain it against a 1 % agar substrate while applying axial stretch through a suction pipette on one end and recording whole-cell currents from a patch pipette placed at the other end. This study was one of the first to record whole-cell currents from single CM that were activated by a ~20 % stretch. The reversal potential of ~ -15 mV was consistent with a more or less non-selective cationic current (Sasaki et al. 1992). From there, a double-barreled glass pipette suction system was developed from pulling and fire-polishing two capillary tubes of one small internal (3-5 µm) and a larger outer diameter (10-15 µm) and sliding one over the other. Attaching this system to a force transducer and coating it with a biocompatible adhesive (Cell-Tak, based on barnacle adhesive proteins) at the tip facilitated CM adhesion (Palmer et al. 1996). This system allowed to suck in the

terminal about eight sarcomere length portion into two such pipettes at both ends, thus allowing to assess passive resting length-tension curves between sarcomere lengths of 1.9 µm and 3.2 µm in skinned CM (Palmer et al. 1996). Zeng et al. (2000) further optimized this double-barrel technique by focusing on a large variety of adhesive coatings, ranging from epoxy raisins, cyanoacrylate glues, silicones, and silanes, with the best choice represented by a combination of silane layer application, followed by amino dendrimer and methyl alcohol treatment after curing. With this approach, non-inactivating inward cation currents that increased action potential duration and were Gd^{3+}-sensitive were recorded during axial stretch, demonstrating a hallmark of mechano-electrical feedback (Zeng et al. 2000) **(Fig. 3A)**. Interestingly, in a study using frog ventricular CM attached to glass pipettes, axial stretch failed to produce robust lengthening of action potential duration in most cells, arguing against a strong MEF, at least in amphibians (Riemer & Tung 2003, see also Tung & Zou 1995).

The fabrication of glass capillaries as described above represents a major technical constraint to many mechanobiology labs. It also involves extensive expertise and training, also limiting experimental throughput. Thus, a parallel development involved carbon-fibre technology to circumvent the need for sophisticated glass and adhesive processing **(Fig. 3B)**. Le Guennec et al. (1990) were among the first to use thin 12 µm diameter carbon fibres that were produced by high temperature treatment of polyacrilonitryl and oxidized to produce free carboxyl groups. Those render carbon tubes sticky to cell membranes, probably by interactions with surface membrane amino groups. This approach allowed spontaneous attachment of carbon fibres of known stiffness to either end of the CM (one compliant fibre for force sensing, e.g. 0.25 N/m, and one stiff fibre for myocyte stretching, e.g. 0.0125 N/m) perpendicularly to the CM long axis upon touching the CM membrane. This allowed to obtain resting length-tension curves and active tension recordings in about 80 % of CM, withstanding active forces of up to ~0.25 mN/mm² at resting length L_0 and ~0.35 mN/mm² at 105 % L_0 stretch (Le Guennec et al. 1990).

In order to obtain even tighter attachment, graphite-reinforced carbon (GRC) fibres of higher stiffness were processed by carbonization of rod-shaped graphite granules and resin oligomer mixtures (Yasuda et al. 2001). A higher stiffness is desirable in

force transducing systems to allow recording of higher forces at a small displacements, and to increase the sensing range, according to Hooke's law (Neuman et al. 2007). Using this enhanced overall stiffness of GRC fibres (>1 N/m), peak isometric forces of ~40 mN/mm² in single rat ventricular myocytes could be successfully recorded (Nishimura et al. 2004). Attaching the GRC fibres provides a high success rate with minimal damage to the cell membrane. No additional adhesive was required, and the technique was successfully implemented in conjunction with electrophysiology and fluorescence microscopy in stretched CMs (reviewed in Nishimura et al. 2008). While the older technique with carbon fibres allowed stretch of single CM up to ~2.1 µm sarcomere length (SL) before rupture (Gannier et al. 1994), the graphite-reinforced carbon fibres allowed going to SL of at least 2.4 µm (Nishimura et al. 2006). While the former study demonstrated that 6 % axial stretch already resulted in a large increase in indo-1 [Ca^{2+}] fluorescence in guinea pig ventricular myocytes (Gannier et al. 1994), the latter is worth mentioning for demonstrating stretch-induced membrane depolarization in quiescent rat ventricular CM, prolonging the late phase of the action potential in beating CMs using ratiometric optical recording of membrane potential with the fast voltage sensitive dye di8-ANEPPS (Nishimura et al. 2006). This can be regarded as another direct demonstration of MEF in CM. Another study in guinea pig ventricular CM attached to carbon fibres and stretched by approx. 9 % confirmed streptomycin-sensitive prolongation of action potential duration and a cationic inward current. The prolonged action potential was carried by MSC-mediated Ca^{2+} influx, as it was abolished by strongly buffering $[Ca^{2+}]_i$ with BAPTA-AM (Belus & White 2003) **(Fig. 3A)**.

To further substantiate the role of axial stretch in modulating ventricular CM intracellular Ca^{2+} homeostasis, varying diastolic pre-loads were applied to single CM via carbon fibre attachment and rest-decay dynamics of sarcoplasmic reticulum [Ca^{2+}] calculated. This was done by comparing cytosolic fura-2 fluorescence in cells exposed or not exposed to diastolic stretch for different durations. In addition, SR Ca^{2+} reloading during different stretches following initial caffeine-induced SR Ca^{2+} depletion was also assessed (Iribe & Kohl 2008). The authors found diastolic axial stretch to both enhance SR Ca^{2+} leak and sarcolemmal Ca^{2+} influx in order to match required Ca^{2+} levels and force production to increased diastolic pre-load in ventricular CM on a beat-to-beat basis. This was subsequently confirmed by assessing diastolic

Ca^{2+} spark rate in carbon fibre axially-stretched ventricular CM. ~8 % stretch caused an acute ~33 % increase in spark rate within 5 s, followed by a return to baseline at sustained distension within 1 min (Iribe et al. 2009). Very interestingly, neither block of mechanosensitive ion channels with GsMTx-4, nor removal of extracellular Na^+ or Ca^{2+}, nor NO synthase inhibition abolished the stretch-induced increase in spark rate, but interfering with cytoskeletal integrity using colchicine did. This suggests that the stretch biosensor, at least for modulating ryanodine receptor (RyR) functions, lies within the cytoskeleton (Iribe et al. 2009). The mechanism of this 'mechano-chemical' coupling in the working heart was subsequently elucidated to be due to axial stretch activating NADP oxidase 2 (NOX2) to generate reactive oxygen species (ROS) in the sarcolemmal and tubular membrane thus, sensitizing nearby RyRs to become leaky (Prosser et al. 2011). This microtubule-dependent sensor-actuator axis, subsequently termed 'X-ROS signaling' was used to explain diastolic arrhythmogenic Ca^{2+} wave initiation in mechanically load-challenged CM (Prosser et al. 2013, 2011). Using cyclic stretch of CMs attached to glass micro-rods coated with the hitherto biological adhesive MyoTak™ (World Precision Instruments, Sarasota, FL, USA), Prosser et al. finally documented that the mechanosensor machinery in ventricular CM was able to differentiate static sustained stretch from more physiologically occurring cyclic stretch regimes. The former confirmed the previously described transient induction of ROS, while the latter induced a steady-state elevation of ROS (Prosser et al. 2013a). Since Prosser et al. used glass micro-rods rather than GRC fibres, their stretch was usually restricted to ~10 % in CM.

Another way to increase stretch range in isolated CM using conventional carbon fibres was introduced by a new carbon fibre 'gripping' technique where both ends of a CM are tightly squeezed between a pair of carbon fibres approaching the cell ends from above and below (Iribe et al. 2014). Using this system, single CM could be stretched to about 2.2 µm (~15 % stretch) without detachment (Iribe et al. 2014).

Similar to the considerations from the previous sections, the carbon fibre techniques reviewed here also suffer from a very limited throughput since only one cell at a time can be handled.

3.7. Elastomer membrane based stretch systems to apply planar stretch to cells (Fig. 4)

The axial end-to-end traction approach presented in **section 3.6.** has some profound limitations: (i) for cells even smaller than CM and not elongated, for instance EC, point attachment is not readily feasible (we are not aware of any study that has successfully implemented dual carbon fibre stretch in EC), (ii) throughput is limited to one cell per attachment and thus, data collection is time consuming, and more severely limiting, (iii) the preparation still does not reflect the situation of multiaxial stretch distributing within tissues. In particular with regard to (iii), simultaneous axial and lateral stretch (with respect to the long and short axis of CM, respectively) distributes along all membrane and cytoskeletal components anchored to the extracellular matrix (ECM) via FAC. One has to reconcile that, in particular in the scenario of isolated CM subjected to exclusive axial rod-rod stretch (see above), cells have been isolated and kept submerged in physiological saline solutions without being able to establish FAC-ECM contacts. Thus, although such approaches represent elaborate and elegant ways to stretch single CM, it is more so in an acute setting of stretch-induced ion channel or fast signaling studies rather than including a natural membrane-mediated anchorage to external surfaces to the conditioning. Also, axial stretch (along the longitudinal CM axis) may not represent the wall tension profiles experienced in hollow organs where filling pressures induce more multiaxial anisotropic or isotropic strain to the cell membrane (Friedrich et al. 2012, Gopalan et al. 2003). Mainly for reasons (i) and (ii), alternative approaches were already developed almost 40 years ago by employing flexible elastomer-polymer substrates on which cells grown could be stretched (Vandenburgh & Kaufman 1979).

3.7.1. Stretch mode definitions with flexible membrane substrates

For the following sections, it is important to reconcile that stretch conferred via planar substrates rather than point-to-point stretch in carbon fibre or glass rod settings (see above) defines different stretch modes. Clamping a flexible rectangular elastomer membrane on opposite sides and applying stretch is referred to as *uniaxial stretch*. It does not necessarily coincide with the main axis of elongated cells (e.g. CM, muscle fibres) adhered to the elastomer surface via FAC-connections, since cells may be oriented randomly if no patterned surfaces were involved. Thus, uniaxial stretch involving elastomer substrates is different from ‘axial stretch’ applied in the techniques discussed before (i.e. **section 3.6.**). Preservation of volume of a flexible membrane during stretch predicts a shortening of the other two Euclidian degrees of

freedom, i.e. a reduction in thickness and width of the membrane. When also the other two rims of the rectangular membrane are clamped by an independent actuator and stretched, this defines a second stretch axis at 90 ° to the other one. This setting is referred to as *biaxial*. Stretch profiles can be equi-biaxial with exact same amplitudes in both planar degrees of freedom or involve different stretch amplitudes. The former results in a more isotropic displacement of the membrane while the latter represents a non-isotropic stretch with complex patterns, depending on the relative amplitudes. *Isotropic* membrane stretch is most accurately represented by equi-multiaxial or radial displacement of circular elastomer membranes, technologies which will be described below. In any case, in biaxial (rectangular membranes) or multiaxial (circular membranes) stretch, the substrate membrane will become thinner with stretch, as this is the only remaining degree of freedom to keep volume constant, which may hamper microscopy due to z-focus shifts during stretch.

3.7.2. Silicon-based elastomer substrate developments and cell-substrate junction

Among the first flexible substrates were silicon rubber sealants that polymerized at air when squeezed from a tube into pre-formed polyethylene casts and subsequently cut into shape, attached to steel clips and stretched via nylon threads through a culture flask by a stepper motor (Buck 1980). That study was also one of the first to demonstrate reorientation of fibroblasts with their long axis perpendicular to the strain axis following repeated uniaxial stretch in order to minimize their strain exposure (Buck 1980). In the following years, silicone became the material of choice to the young ‘cell stretch community’ using the same silane materials as in medicinal applications, e.g. examination gloves. *Dow Corning* was already a leading company in this area at that time and has expanded its position by a vast number of elastomer materials on the market, the most important being polydimethyl-siloxane (PDMS), widely used in medical research, tissue engineering and mechanobiology today. In the early days, stretch chamber were assembled from custom-cut substrate geometries of ‘silastic membranes’ (Dow Corning Corp., Medical Products, Midland, MI, USA) and glued or clamped to Perspex holders or metal clamps attached to actuators for extension. These were also the times in the 90s when researchers started to play with different coatings for stronger attachment of cells to substrates.

About the same time, the processing of silanic membranes to increase hydrophilicity and promote cell adherence was advanced through gas plasma technologies, where oxidation of the hydrophobic membrane using cold gas plasma was shown to functionally increase wettability of silanes for up to 72 h. Although this technique is still used today, it is restricted to few labs holding gas plasma equipment. Consequently, chemical etching surface treatments employing e.g. peroxide, have been developed (Zhou et al. 2012). Another advantage of custom-made PDMS elastomers nowadays is given by the fact that their resulting stiffness can be modulated by varying base compound – catalyzer ratios (Shi et al. 2013). Substrate stiffness is a crucial parameter for cells to tightly adhere to and establish focal adhesion connections with the substrate, as previously shown for CM where a substrate stiffness of ~25 kPa was found optimal for vinculin and α-actin expression in CM grown on static substrates (Galie et al. 2013). On those intermediate stiffness substrates, ß1-integrins were distributed homogeneously across CM but did not colocalize to the z-disk, while in stiff (255 KPa) and compliant (7 KPa) environments, they span the entire z-disk region (Galie et al. 2013). This supports the notion that cells 'sense' their mechanical environment and react accordingly with the formation of FACs. On the contrary, it also means that the elastomer stretch can only be transduced to the cell membrane, if the connection between adhered cells and elastomer substrate was tight, i.e. depending on the establishment of FACs with the elastomer substrate. Since FACs 'reach out' to ECM components, elastomer substrates have been successively coated with ECM proteins to promote adhesion, e.g. using laminin, fibronectin, or RGD-(Arg-Gly-Asp)-peptide sequences. As detailed later in this section, the tightness of this cell-ECM junction requires calibration for each cell type and coating, which has been often ignored in the literature.

Elastomer membrane systems, although not all designed for high-throughput, are per definition suited for high-content analyses, since many cells adhered to the elastomer membrane and subjected to stretch, can be simultaneously read-out.

3.8. Pneumatic actuation systems and optimizations for throughput and microscopy

An approach to membrane actuation was conceptualized and implemented by Albert Banes who developed pneumatic-systems for elastomer membrane stretch

applications that ultimately resulted in the foundation of *FlexCell Int. Corp.* (Burlington, NC, USA) which is still the market leader in providing pneumatic stretch systems for mechanobiology. In a narrative review from 2013, Albert Banes very nicely summarizes the past of pneumatic cell stretch systems and translation from basic research to entrepreneurship, and a read-through is highly recommended (Banes 2013). Between 1980 and 1985, he developed the idea of growing cells on flexible elastomer substrates and stretching them by bending the membrane from below through pneumatic suction **(Fig. 4A)** which became the first biomedically engineered design of the Flex I® and BioFlex® flexible bottom culture plates (Banes 2013). According to the nomenclature of stretch modus of **3.7.1.**, pneumatic membrane inflation-deflation actuation represents an isotropic stretch regime, if no further guidance geometries, e.g. pillars are involved (see below).

The original design of radial extension of the elastomer substrate through suction precludes its application to live-cell imaging due to marked z-plane shifts during stretch protocols. This is why almost exclusively all such approaches employed post-stretch optical assessment on either fixed cells or on the non-stretched membrane for focussing (Dhein et al. 2014, Wang et al. 2013, Tan et al. 2008, Garvin et al. 2003) rather than live-cell imaging (De Jonge et al. 2013).

The *FlexCell TissueTrain® Culture Plate* was a further development trying to minimize membrane z-shifts by applying pneumatic suction to suck in the membrane between the walls of a central Teflon loading post and an outer wall. While the membrane was uniaxially stretched over the surface of the loading post, it remained in the same horizontal plane (Dhein et al. 2014, Banes 2013, Garvin et al. 2003). Still, most imaging research using this system has been conducted on post-stretch cells, either fixed or native, but not during stretch. For instance, Dick et al. (2013) used that system to stretch pulmonary artery smooth muscle cells on collagen-coated PDMS membranes applying 10 % or 20 % cyclic (0.5 Hz duty cycle) uniaxial stretch for 24 h and found supra-physiological (20 %) stretch to increase peroxynitrite formation (visualized by dihydroethidium fluorescence) and immunoreactive nitrotyrosine detection. Of note, the *TissueTrain® Culture Plate* system also increases throughput by employing parallel culture wells subjected to pneumatic suction.

In addition, in the above-mentioned design, the thick loading post material from below largely prevents inverted microscopy through water immersion, apart from lubricants between loading post and elastomer membrane introducing refractive index mismatch (Kreutzer et al. 2014). To optimize these constraints, Kreutzer et al. (2014) introduced an improved pneumatic circular equi-axial or isotropic actuating system consisting of a thin PDMS membrane, an outer and inner PDMS shell and a rigid glass plate **(Fig. 4A)**. Applying negative pressure in the space between the shells, the PDMS membrane was deformed and the inner shell symmetrically buckled in radial directions. Since this design did not involve any solid loading post underneath the PDMS membrane from below, inverted microscopy was accessible (Kreutzer et al. 2014). Still, calibration of in-plane strain by pressure and z-displacement of the elastomer membrane yielded a large focus shift of 300 µm at 10 % strain which requires time-consuming focus readjustments upon applying stretch **(Fig. 4A, right panel)**. Applying this system to human pluripotent stem cells (hPSC) grown on gelatin-coated PDMS substrates and following differentiation into CM, cyclic long-term equi-axial (or isotropic) stretch increased expression of Myh7 and Trop I, as assessed by qPCR after 21 d of stretch. That study did not employ any imaging attempts of hPSC-derived CM, probably because of optical constraints (Kreutzer et al. 2014). The system as described is not suitable for high-throughput screening, as only one stretch-well was involved.

In another pneumatically-actuated approach, Wang et al. (2010) designed a vacuum chamber within a thick PDMS layer of vertical support walls connected to a thin PDMS membrane of 50 µm thickness bulging down over a cover-slip to which adhesive connection was established by introducing a silicone oil layer. Suction was established from the side through the PDMS wall, sucking the buckling PDMS membrane portion to the wall and stretching the portion adhered to the cover slip in either uni- or equi-axial (isotropic) fashion. This way, focal membrane shifts could be minimised for high NA immersion microscopy on an inverted microscope. Although quantification of the focal shifts were not given, the authors were able to provide high-resolution confocal images of EGFP-expressing fibroblasts adhered to the PDMS to visualise actin stress fibre dynamics in single cells during a whole stretch-relaxation cycle (Wang et al. 2010). The system, as described, is not suitable for high-throughput screening but may, in principle, be parallelized in the future.

3.9. Mechanically actuated elastomer systems and optimizations for high-throughput and microscopy

Alternative to pneumatically-operated stretch systems, the majority of past and recent developments has originated from biomedical engineering of mechanical actuator systems. The most commonly used approach is to use rectangular PDMS cast chambers of thick support walls with holes to connect to prongs or clamps situated on side-base plates and a thin (~50 µm) bottom **(Fig. 4B)**. Such chambers can be cast with appropriate molds, seeded with cells on the ECM-protein coated bottom and attached to clamps that are then driven by linear stepper motor or piezo-driven actuators.

In 1988, Herman Vandenburgh presented a computerized mechanical cell stimulator for tissue culture that also already went into the high-throughput direction by employing 24-well cell growth chambers of sandwich-design. This consisted of a 24-holes steel base plate onto which prongs of defined heights could be inserted. Over those prongs a corresponding Teflon chamber was placed to which a silastic membrane was glued on the bottom. Inserting silicone gaskets into these small 24 well chambers and coating with rat tail collagen solution, cells could be seeded in each well and assembled with the underlying prong metal plate to a stepper motor. Each prong acted as a piston that was impressed onto the silastic membrane, thus stretching the membrane and the attached cells. The design of modular attachment of prongs also allowed to include control wells that had no prong underneath and were thus, not stretched by the actuation (Vandenburgh 1988). Using this system with primary avian skeletal muscle myoblasts, continuous stretch-relaxation cycles promoted faster fusion and reorientation of myotubes with their long axis perpendicular to the strain direction (Vandenburgh & Karlisch 1989, Vandenburgh 1988). This elastomer-membrane indentation-induced stretch acted as a role model for many subsequent developments. Of note, this system subsequently was used to study the adhesion and orientation behavior of adult rat ventricular CM on laminin-coated silastic membrane before, during or after continuous cyclic uniaxial stretch. The authors described continuous uniaxial stretch during the cell seeding period to be optimal for attachment and orientation of CM parallel to the stretch direction, which seems to be a fundamentally different behavior to fibroblasts and myotubes (Samuel & Vandenburgh 1990). Moreover, CM maintained their new orientation and

rod shape over several days, making stretch-induced long-term culture of CM an interesting model to inhibit or prolong the effect of dedifferentiation of mammalian CM otherwise seen in static long-term cultures (Zhang et al. 2010).

3.9.1. Uniaxially-actuated elastomer membrane stretch systems

Uniaxial stretch systems, such as successively developed, e.g. by Matsumoto et al. (1996) **(Fig. 4B)** or Yost et al. (2000), not only served as stimulations for ongoing improvements, but were also subsequently commercialized by Biotech companies, e.g. *Strex Inc.* in Osaka (www.strexcell.com), who also vastly contribute to parallelization of multiple chambers within the same stretch actuation cycle to increase throughput. In the early design given by Yost et al. (2000), the stretch unit was designed as a dual stretch-actuator for two culture dishes simultaneously. Silicone rubber membranes of 250 µm thickness clamped into poly-ether-etherketone (PEEK) rods by polytetrafluorethylene (PTFE) snap-on clamps were displaced by a stepper motor. Stretching neonatal cardiac fibroblasts on collagen-coated membranes (0 – 12 % stretch, 0 – 10 cyc/min), ß$_1$-integrin formation, as analyzed by blot analysis post-stretch, increased for 3 % stretches but decreased for larger stretches (Yost et al. 2000).

Using a similar design, uniaxial cyclic strain was found to regulate cell alignment and motility in EC. In particular, adhered HUVEC cells oriented perpendicular to the major strain axis in monolayers, and in 3D cultures, strain regulated the directionality of sprouting (Matsumoto et al. 2007). However, due to the elastomer membrane over a non-transparent base-plate **(Fig. 4B)**, imaging was performed post-stretch in fixed cells. Connections between uniaxial stretch on HUVEC cells and Ca^{2+} entry were studied using a commercially stretch apparatus by *Strex Inc.* that does not involve base plates underneath the PDMS chamber, but allows the free-hanging part of the chamber to be accessed with objective lenses from below (Ito et al. 2010). HUVEC adhered to fibronectin-coated elastomers were uniaxially stretched by stretching the polymer membrane 10% - 30%. During short (3 s) stretches, global fura-2 Ca^{2+} fluorescence increased and then slowly decayed upon relaxation. This decay was dependent on stretch amplitude, external Ca^{2+} and was blocked by Gd^{3+} and ruthenium red, a TRPV channel blocker (Ito et al. 2010). Disruption of actin cytoskeleton with cytochalasin D inhibited stretch-induced Ca^{2+} entry. This argued in

favor of a modulation of external Ca^{2+} entry through TRPV channels by the cytoskeleton, a mechanism that is different from store-operated Ca^{2+} entry in HUVEC cells (Ito et al. 2010).

Another recent study employed the same system to subject human embryonic stem cell (ESC)-derived CM on matrigel-coated silicone chamber to cyclic uniaxial stretch (10 – 30 % elongation at 1 Hz) (Qi et al. 2015). The authors observed a longitudinal stretch-induced rise in $[Ca^{2+}]_i$ that was inhibited by the TRPV4 antagonist 4α-phorbol-12,13-didecanoate. In addition, uniaxial stretch for 2 h induced realignment of hESC-CMs transverse to the stretch direction which also was abolished by the antagonist. That study indicated an important function of cardiac TRPV4 as a biomechanosensor to mediate reorientation patterning against external mechanical stress (Qi et al. 2015).

3.9.2. Multiaxially-actuated elastomer membrane stretch systems

As mentioned before, in hollow organs, filling pressure concentrically acts on organ walls thus, ideally translating an isotropic stretch profile to the wall elements. Depending on local wall geometries, such strain profiles may also be anisotropic. In particular, the anisotropicity of the stress-strain relationship in two axes, i.e. longitudinal versus lateral, when considering elongated cell such as muscle or CM, depends on the compliance values of the material and the cells rather than the strain translation method. Even if strain was applied totally isotropically to a substrate membrane, the membrane of cells would not be expected to be stretched to the same extents in different directions. This is in particular the case for CM or muscle cells with their dedicated longitudinal and lateral arrangement of different cytoskeletal and anchorage proteins exerting their respective mechanical compliances. For CM, uniaxial stretch may not be the most physiological stimulus. Stretch on their distinct, almost perpendicularly arranged membranes systems, i.e. sarcolemma and tubules, may be translated differently under multiaxial stretch regimes. While under uniaxial stretch, sarcolemmal mechanosensitive elements become stretched, in the tubules, they are expected to become slack from considerations of cell volume remaining constant during acute stretch **(Fig. 5A)**. Under isotropic stretch (or anisotropic multiaxial stretch, in case of non-equiaxial stretch), we hypothesize a stretch to both membrane systems, initiating a more vigorous and maybe different

mechanotransduction cascade in order to adapt FAC anchorage. In particular, the latter must be embedded in cellular feedback signaling cascades which should involve MSC (i.e. TRPC channels) and nuclear FAC gene activation cascades triggered by the MSC-induced Ca^{2+} influx, as visualized by a proposed work hypothesis of ours **(Fig. 5B)**.

To implement mechanically-actuated multiaxial stretch, early designs included motor-driven indentation of Teflon-made plates underneath a culture dish, the bottom of which was sealed with a silastic membrane, and displaced sinusoidally by a speed-controlled motor-driven cam (Cheng et al. 1998). Through this translation, a homogeneous and uniform equi-biaxial stretch could be applied to adhered human VSMC and release of fibroblast growth factor-2 from VSMC was stretch-dependently detected (Cheng et al. 1998). In a related study, the same authors also attached neonatal rat CM to this system and found equi-biaxial or isotropic stretch to suppress inducible NO synthase expression (Yamamoto et al. 1998). Although their system provided isotropic stretch, the mechanical actuator sub-construction prevented image acquisition so that all data given were from post-stretch protein biochemistry.

A subsequent design by Rana et al. (2008) aimed to increase equi-biaxial stretch throughput by arranging several PVC discs on a Perspex bottom plate onto which another top-plate containing wells with a Bioflex Collagen Plate I (Flexcell®) elastomer bottom were lowered for indentation. Stretching neonatal rat atrial CM showed stretch-dependent upregulation of e.g., calcineurin, calcineurin-interacting protein 1, voltage-gated $K_V4.2$ however, again, not involving direct optical readout technologies (Rana et al. 2008).

Huang et al. (2010) designed a vertically actuated system pushing an indenter ring against a horizontal PDMS membrane **(Fig. 6A)**. The modular indenter design allowed switching between equiaxial ('equi-biaxial' in their nomenclature, but in fact equi-multiaxial or isotropic since a circular indenter ring was used) and uniaxial strain profiles (Huang et al. 2010), as verified by fluorescent bead displacements **(Fig. 6A)**. Using EGFP-vimentin labelled bovine aortic EC on fibronectin-coated elastic membrane, 15 min of cyclic isotropic stretch resulted in a much larger number of FAC to the substrate as compared to uniaxial stretch, where FAC were retracted (Huang et al. 2010). Although not explicitly given in that paper, the authors indicated that

'*continuous observation of cells cultured on the elastic membrane is possible since the focal distance remains effectively constant during the stretch process*' (Huang et al. 2010).

Before the aforementioned study, biomedical engineers had also combined photolithographic and microfluidics techniques to micro-pattern extracellular matrices in parallel lines on deformable silicone elastomers to produce aligned confluent myocytes derived from neonatal ventricular CM. An elliptical stretcher applying 2:1 axis ratio anisotropic biaxial stretch (but not *equi-biaxial*) was applied through an indenter on an elastomer membrane to produce main strain either parallel or perpendicular to the myocyte long axis (Gopalan et al. 2003). Sarcomere organization, hypertrophy and cell-to-cell junctions were more markedly remodelled by transverse over longitudinal anisotropic stretch (Gopalan et al. 2003). This argues in favour of the hypothesis that sarcolemma and perpendicular t-tubular membranes are differentially involved in mechanosensing and –regulation.

In order to be able to produce fast isotropic cell stretch to cells with a minimum z-shift suitable for live-cell imaging, Rapalo et al. (2015) and ourselves (Schürmann et al. 2016), almost at the same time, developed novel isotropic cell stretch devices. Rapalo et al. (2015) presented an in-plane mechanical stretch device utilizing six evenly spaced clamps attached to a flexible large culture dish-cast membrane allowing a maximum linear strain of 20 %. Isotropic membrane strain (in this case, equi-triaxial stretch) was linearly translated to human bronchial epithelial cells adhered on collagen-I coated PDMS dishes, as judged from linear distance measurements of DAPI stained nuclei under a confocal microscope pre- and post-stretch (Rapalo et al. 2015). However, the actual increase in cell membrane area by applying defined isotropic stretch was not assessed. However, this is important since the confirmation of 1:1 cell membrane area increase to PDMS membrane area increase is crucial to verify transmission efficiency of PDMS membrane stretch to the cell membrane. This is strongly dependent on the tightness of mechanical linkage between the two membrane boundaries.

In order to provide a tool for studying the link in the biosensor-bioactuator cycle of mechanosensing and FAC-remodelling in future studies **(Fig. 5B)**, we sought to (i) build a compact isotropic stretch system fitting on all commercial microscope stages,

and to (ii) calibrate stretch-strain relationships at the level of the cell membrane using cell membrane border detection rather than at the level of the PDMS membrane using fluorescent beads within the substrate. Our so-called *IsoStretcher* **(Fig. 6B)** uses a rotational-to-radial translation of a V-belt driven outer ring connected to six evenly spaced hooks in a radial guidance groove connected via an intermediate translation ring. The mechanism of translating rotation to radial displacement is implemented via oblique grooves in the intermediate transmission ring thus, allowing actuation via a fine-tuned swivel motor (Schürmann et al. 2016). Besides confirmation of isotropicity (here: equi-triaxial stretch, **Fig. 6Bii**), we applied the system to several cell lines so far, including HEK293, HeLa cells and murine cardiac immortalised HL-1 cells, to name a few. The system proved adequate to monitor stretch-dependent Ca^{2+}-entry in HL-1 cells.

Although suitable for high-content screening through live-cell imaging (i.e. many cells per stretched elastomer), all systems described in this section have not yet been improved in their design to implement high-throughput screening (i.e. parallelization of assays). However, since most those newly engineered systems are recent inventions, ongoing engineering might address this need in the future.

One important calibration that needs to be assessed for every cell line and coating on PDMS membranes is actually the reliability of the hardware strain transmission to the cell membrane (see above). If only few FAC were established with the PDMS membrane, mechanical linkage to the substrate would be loose and not transferred to the cell membrane. Consider a cell floating on the substrate with no FAC established. Without confirmation of actual cell membrane distension with applied stretch, one would simply stretch the substrate underneath the cells, wrongly assuming the lack of cell reaction to stretch being a lack of mechano-signaling, while in fact, stretch to the cell membrane did not occur at all. Therefore, we now provide a method to verify cell membrane stretch with PDMS membrane stretch such as given for HEK cells (Schürmann et al. 2016) **(Fig. 6B iii)**. For HEK cells, we can assume cells to follow hardware stretch up to ~17 %, from which they fall behind and eventually detach. We have used this approach here in Piezo1-transfected HEK293 cells (see Methods) to demonstrate the mechanosensitivity of Piezo1 and subsequent Ca^{2+} entry **(Fig. 7A)**. HEK293 cells stably expressing a Piezo1-mCherry construct were subjected to

isotropic stretch on a fibronectin-coated custom-cast PDMS membrane, demonstrating an instantaneous almost four-fold increase in Fluo-4 Ca^{2+}-fluorescence that slowly declined again during maintained stretch, and rapidly returned to baseline fluorescence upon de-stretching **(Fig. 7A)**. In conjunction with a recent study on the direct mechanosensitivity of Piezo1 (Syeda et al. 2016), our novel results here also demonstrate direct mechanosensitivity in a heterologous expression system responding to isotropic planar stretch.

3.10. Adding dimension: more physiological stretch conditions in adult CM can be modelled through 3D hydrogel culture (*'cell-in-a-gel'* approach)

Planar stretch of adult CM coated on flexible membranes is very poorly covered in the literature. Since the early work by Vandenburgh & Karlisch (1989), we are not aware of any study that has successfully stretched adult ventricular CM on flexible substrates (i) to such and exceeding extents as given by the stretch approaches using glass pipettes or carbon fibre rods (see above) and, (ii) actually confirming the applied substrate stretch translation to cell membrane area distension. We know of several strenuous unsuccessful attempts within the community (personal communications), including by our own group, to optimize several coatings, including use of fibronectin, laminin, gelatin, collagen or matrigel, and their combination, with limited success.

Although adhering to coated PDMS substrates, adult CM do not seem to establish sufficient FAC anchorage with the planar substrate to prevent their detachment already upon 3 – 5 % stretch (unpublished observations). As visualized in **Fig. 5A**, we think there is a fundamental difference in anchorage efficiency between 2D for CM coated on planar substrates and CM embedded in tissue where FAC-ECM anchorage takes place in 3D. Searching for appropriate hydrogel embedding procedures, we came across a recent approach introduced as *'cell-in-a-gel'* by Jian et al. (2014) who embedded single adult ventricular CM in polyvinyl-alcohol (PVA) based hydrogels that can also be doped with RGD-peptide sequences for advanced anchorage to FAC. Those peptide sequences act as a binding substrate for integrins (Bacakova et al. 2007). This way, the embedded CM finds a binding substrate to establish FAC in all directions. Using this approach, an intact ec-coupling was demonstrated. Furthermore, increased gel stiffness caused afterload to increase,

which was answered by increased systolic Ca^{2+} transients within the gel to counteract on mechanical load (Jian et al. 2014).

Since the aforementioned study did not include any stretch, we adopted PVA-hydrogel embedding in conjunction with our *IsoStretcher* and embedded adult mouse ventricular CM in mechanically weak (compliant, Young modulus E~1 kPa), medium (E~4-9 kPa) and strong (stiff, E>10 kPa) gels (details see Methods), depending on the total amount of thiol groups in the hydrogel **(Fig. 7B)**. **Fig. 7B (i)** shows images from a stretch-sequence following a single CM during isotropic stretch from 0 to 15 % alongside with cell border detection (right panel) confirming an increase in cell membrane area in both axes. This increase was larger in longitudinal versus lateral direction in terms of absolute displacement (~12 µm vs. ~2 µm, respectively) in the shown CM. **Fig. 7B (ii)** shows the results from several gels of different stiffness, demonstrating that CM in weak gels did not follow substrate stretch at all while they followed an almost 1:1 transmission in strong gels and fell somewhat behind in intermediate gels. This is a very novel finding and important since it demonstrates that the stiffness of the hydrogel must be larger than the stiffness of the cell to stretch. From a biophysical standpoint, this makes perfect sense: in a connection of elastic elements in series, the element with higher compliance will always give in to the applied strain over the less compliant element. In our case, stretching a weak gel, the CMs with a higher stiffness will not be stretched, indicating that the more compliant hydrogel will simply extend to lessen the strain. More importantly, the larger absolute membrane displacement in longitudinal over lateral direction, as seen in the example CM in **(i)**, was not paralleled by the relative displacements in several CM in the gels, which were 13.1 ± 7.1 % lateral over 5.5 ± 5.1 % longitudinal in the medium gels and 9.5 ± 7.2 % lateral over 5.3 ± 5.2 % longitudinal in the strong gels (n between 6 and 7 CM for the gels shown, mean ± SD). This counter-intuitive finding suggests a larger longitudinal passive stiffness over lateral passive stiffness and requires more thorough investigation in future studies. We are not aware of any study that has given lateral versus longitudinal stiffness measurements in isolated adult CM.

Using the strong gels, we started initial experiments embedding single CM and staining the gel with Fluo-4. In Ca^{2+} containing external solution, stretching the gel to

15 % induced a slow increase in Ca^{2+}-fluorescence developing over 10 min and saturating at a level 5 % over baseline as shown in **Fig. 7B (iii)**. This level of stretch-induced Ca^{2+} entry fits very nicely with our previous observation in single rat ventricular CM freely contracting against no afterload on cover slips and stimulated with external field pulses, where we observed a roughly 5 % contribution to Ca^{2+} transients attributable to MSC by comparing transients in the absence and presence of GsMTx-4 (Friedrich et al. 2012). This contribution during unloaded contraction should be attributable to activation of MSC in the tubular membrane upon shortening (Friedrich et al. 2012) while the present results in 3D stretching adult CMs should reflect activation of MSC activation in both sarcolemma and tubules **(see Fig. 5A)**. This approach represents a useful tool to address the cellular actuation loop involving membrane stretch sensors to FAC remodelling under static or cyclic isotropic stretch profiles in future studies, in particular deciphering the underlying signalling mechanisms downstream to Ca^{2+} influx **(Fig. 5B)**.

4. Concluding remarks

In this paper, we present an overview on the involvement of mechanosensitive ion channels and mechano-biosensors in the regulation and homeostasis of both cardiac and vascular cells. In mammals, TRP channels have been extensively investigated, and it is sometimes difficult to stay on top of new findings while for Piezo channels, evidence of their role in the cardiovascular system is just emerging. Nevertheless, it is crucial to reconcile the biomedically engineered technologies available for mechanobiology and highlight their strengths but also their limitations. In general, a more robust nomenclature regarding the type of stretch applied to the cells is needed. We have summarized the distinct differences between uniaxial and multiaxial stretch. In the latter, while actuation of axes is equal (equi-biaxial, -triaxial, etc.), resulting in isotropic membrane displacements, non-equal actuation of stretch axes can be used to study anisotropic multiaxial stretch profiles.

Although we have gained fundamental mechanistic insights into mechano-signalling from 2D approaches, the literature, and also our own observations, point towards the direction that adult cardiomyocytes are particularly cumbersome to be forced into a sufficient 2D adhesion environment. It also makes sense from biophysical

considerations that uniaxial stretch will have different effects in particular to elongated cells (cardiomyocytes, fibroblasts, etc.) than multiaxial stretch approaches, whether they are isotropic or anisotropic.

'Seeing is believing', and in order to elucidate spatial and temporal reactions of cells to mechanical stress, new technologies are required from biomedical engineering, for instance to accommodate cell-stretch systems with high-resolution microscopy devices. We here present novel data using our *IsoStretcher* technology in order to verify mechanosensitivity of Piezo1 expressed in heterologous HEK293 cells in 2D and Ca^{2+} entry into adult normal mouse ventricular CM embedded into hydrogels in 3D by microscopy. These results build the proof-of-concept for future studies taking a deeper look into the differential effects of 2D versus 3D mechanotransduction and also to close the biosensor-bioactuator loop of cellular anchorage within ECM matrix, as suggested in **Fig. 5B**. On a side note, the novel stretch technologies presented may not only provide a wealth of applications for the mechanotransduction community, but also a useful tool for the stem cell community to induce and promote stem cell differentiation by stretch (e.g. Paul et al. 2017, Qi et al. 2015).

Acknowledgements. This project was funded by mobility grants from the German Academic Exchange Service DAAD (#57214153 to OF) and the Australian Group of Eight (Go8 to BM), by a project grant of the National Health and Medical Research Council (NHMRC APP1108013 to OF, BM, VN), an NHMRC Principal Research Fellowship (to BM), an NHMRC Program Grant and Senior Research Fellowship (to DF) and a DFG grant (FR2993/23-1 to OF).

References

1. Adapala RK, Thoppil RJ, Luther DJ, Paruchuri S, Meszaros JG, Chilian WM, Thodeti CK (2013) TRPV4 channels mediate cardiac fibroblast differentiation by integrating mechanical and soluble signals. *J Mol Cell Cardiol* 54, 45-52.
2. Alenghat FJ, Fabry B, Tsai KY, Goldmann WH, Ingber DE (2000) Analysis of cell mechanics in single vinulin-deficient cells using a magnetic tweezer. *Biochem Biophys Res Comm* 277, 93-99.
3. Alvarez-Miguel I, Cidad P, Perez-Garcia MT, Lopez-Lopez JR (2017) Differences in TRPC3 and TRPC6 channels assembly in mesenteric vascular smooth muscle cells in essential hypertension. *J Physiol* 595(5), 1497-1513.
4. Anderson M, Kim EY, Hagmann H, Benzing T, Dryer SE (2013) Opposing effects of podocin on the gating of podocyte TRPC6 channels evoked by membrane stretch or diacylglycerol. *Am J Physiol Cell Physiol* 305, C276-C289.
5. Bacakova L, Filova E, Kubies D, Machova K, Proks V, Malinova V, Lisa V, Rypacek F (2007) Adhesion and growth of vascular smooth muscle cells in cultures on bioactive RGD peptide-carrying polylactides. *J Mater Sci Mater Med* 18(7), 1317-1323.
6. Balligand JL, Feron O, Dessy C (2009) eNOS activation by physical forces: from short-term regulation of contraction to chronic remodelling of cardiovascular tissue. *Phys Rev* 89, 481-534.
7. Banes AJ (2013) Out of academics: education, entrepreneurship and enterprise. *Ann Biomed Eng* 41(9), 1926-1938.
8. Baumgarten CM, Clemo HF (2003) Swelling-activated chloride channels in cardiac physiology and pathophysiology. *Prog Biophys Mol Biol* 82, 25-42.
9. Bausch AR, Ziemann F, Boulbitch AA, Jacobson K, Sackmann E (1998) Local measurements of viscoelastic parameters of adherent cell surfaces by magnetic bead microrheometry. *Biophys J* 75, 2038-2049.
10. Bavi N, Nakayama Y, Bavi O, Cox CD, Qin QH, Martinac B (2014) Biophysical implications of lipid bilayer rheometry for mechanosensitive channels. Proc Natl Acad Sci USA 111(38), 13864-13869.
11. Beech DJ (2013) Characteristics of transient receptor potential canonical calcium –permeable channels and their relevance to vascular physiology and disease. *Circ J* 77, 570-579.
12. Belus A, White E (2003) Streptomycin and intracellular calcium modulate the response of single guinea-pig ventricular myocytes to axial stretch. *J Physiol* 546.2, 501-509.
13. Bett GCL, Sachs F (2000) Whole-cell mechanosensitive currents in rat ventricular myocytes activated by direct stimulation. *J Membr Biol* 173, 255-263.
14. Bode F, Sachs F, Franz MR (2001) Tarantula peptide inhibits atrial fibrillation. *Nature* 409, 35-36.
15. Borbiro I, Badheka D, Rohacs T (2015) Activation of TRPV1 channels inhibits mechanosensitive Piezo1 channel activity by depleting membrane phosphoinositides. *Sci Signal* 8, ra15.
16. Bowman CL, Gottlieb PA, Suchyna TM, Murphy YK, Sachs F (2007) Mechanosensitive ion channels and the peptide inhibitor GsMTx-4: history, properties, mechanisms and pharmacology. *Toxicon* 49, 249-270.
17. Brady AJ, Tan ST, Ricchiuti NV (1979) Contractile force measured in unskinned isolated rat heart fibres. *Nature Lond* 282, 728-729.
18. Buck RC (1980) Reorientation response of cells to repeated stretch and recoil of the substratum. *Exp Cell Res* 127, 470-474.
19. Cha SK, Kim JH, Huang CL (2013) Flow-induced activation of TRPV5 and TRPV6 channels stimulates Ca(2+) activated K(+) channels causing membrane hyperpolarization. *Biochim Biophys Acta* 1833, 3046-3053.
20. Charras GT, Horton MA (2002) Single cell mechanotransduction and its modulation analysed by atomic force microscope indentation. *Biophys J* 82(6), 2970-2981.
21. Cheng GC, Briggs WH, Gerson DS, Libby P, Grodzinsky AJ, Gray ML, Lee RT (1998) Mechanical strain tightly controls fibroblast growth factor-2 release from cultured human vascular smooth muscle cells. *Circ Res* 80(1), 28-36.

22. Christiakov DA, Orekhov AN, Bobryshev YV (2017) Effects of shear stress on endothelial cells: go with the flow. *Acta Physiologica* 219(2), 382-408.
23. Clemo HF, Stambler BS, Baumgarten CM (1998) Persistent activation of a swelling-activated cation current in ventricular myocytes from dogs with tachycardia-induced congestive heart failure. *Circ Res* 83, 147-157.
24. Codan B, Del Favero G, Martinelli V, Long CS, Mestroni L, Sbaizero O (2014) Exploring the elasticity and adhesion behaviour of cardiac fibroblasts by atomic force microscopy indentation. *Mater Sci Eng C Mater Biol Appl* 40, 427-434.
25. Coste B, Xiao B, Santos JS, Syeda R, Grandl J, Spencer KS, Kim SE, Schmidt M, Mathur J, Dubin AE, Monatl M, Patapoutian A (2012) Piezo proteins are pore-forming subunits of mechanically activated channels. *Nature* 483, 176-181.
26. Cox CD, Bae C, Ziegler L, Hartley S, Nikolova-Krstevski V, Rohde PR, Ng CA, Sachs F, Gottlieb PA, Martinac B (2016) Removal of the mechanoprotective influence of the cytoskeleton reveals Piezo1 is gated by bilayer tension. *Nat Commun* 7, 10366.
27. Davis CA, Zambrano S, Anumolu P, Allen AC, Sonogui L, Moreno MR (2015) Device-based in vitro techniques for mechanical stimulation of vascular cells: a review. *J Biomech Eng* 137(4), 040801.
28. De Jonge N, Baaijens FP, Bouten CV (2013) Engineering fibrin-based tissue constructs from myofibroblasts and application of constraints and strain to induce cell and collagen reorganization. *J Vis Exp* 80, e51009.
29. Demion M, Bois P, Launay P, Guinamard R (2007) TRPM4, a Ca2+-activated nonselective cation channel in mouse sino-atrial cells. *Cardiovasc Res* 73, 531-538.
30. Dhein S, Schreiber A, Steinbach S, Apel D, Salameh A, Schlegel F, Kostelka M, Dohmen PM, Mohr FW (2014) Mechanical control of cell biology. Effects of cyclic mechanical stretch on cardiomyocyte cellular organization. *Prog Biophys Mol Biol* 115(2-3), 93-102.
31. Dick AS, Ivanovska J, Kantores C, Belcastro R, Tanswell AK, Jankov RP (2013) Cyclic stretch stimulates nitric oxide synthase-1-dependent peroxynitrite formation by neonatal rat pulmonary artery smooth muscle. Free Radic Biol Med 61, 310-319.
32. Dietrich A, Gudermann T (2011) TRP channels in the cardiopulmonary vasculature. *Adv Exp Med Biol* 704, 781-810.
33. Dyachenko V, Husse B, Rueckschloss U, Isenberg G (2009) Mechanical deformation of ventricular myocytes modulates both TRPC6 and Kir2.3 channels. *Cell Calcium* 45, 38-54.
34. Earley S, Waldron BJ, Braden JE (2004) Critical role for transient receptor potential channel TRPM4 in myogenic constriction of cerebral arteries. *Circ Res* 95, 922-929.
35. Eder P, Molkentin JD (2011) TRPC channels as effectors of cardiac hypertrophy. *Circ Res* 108, 265-272.
36. Fabiato A, Fabiato E (1975) Dependence of the contractile activation of skinned cardiac cells on the sarcomere length. *Nature Lond* 256, 54-56.
37. Fede C, Fortunati I, Petreeli L, Guidolin D, De Caro R, Ferrante C, Albertin G (2014) An easy-to-handle microfluidic device suitable for immunohistochemical procedures in mammalian cells grown under flow conditions. *Eur J Histochem* 58(2), 2360.
38. Feng SL, Sun MR, Li TT, Yin X, Xu CQ, Sun YH (2011) Activation of calcium-sensing receptor increases TRPC3 expression in rat cardiomyocytes. *Biochem Biophys Res* 406, 278-284.
39. Friedrich O, Wagner S, Battle AR, Schürmann S, Martinac B (2012) Mechano-regulation of the beating heart at the cellular level – mechanosensitive channels in normal and diseased heart. *Prog Biophys Mol Biol* 110(2-3), 226-238.
40. Galie PA, Khalid N, Carnahan KE, Westfall MV, Stegemann JP (2013) substrate stiffness affects sarcomere and costamere structure and electrophysiological function of isolated adult cardiomyocytes. *Cardiovasc Pathol* 22(3), 219-227.
41. Gannier F, White E, Lacampagne A, Garnier D, Le Guennec JY (1994) Streptomycin reverses a large stretch induced increase in $[Ca^{2+}]i$ in isolated guinea pig ventricular myocytes. *Cardiovasc Res* 28, 1193-1198.

42. Garvin J, Qi J, Maloney M, Banes AJ (2003) Novel system for engineering bioartificial tendons and application of mechanical load. *Tissue Eng* 9(5), 967-979.
43. Gomis A, Soriano S, Belmonte C, Viana F (2008) Hypoosmotic- and pressure-induced membrane stretch activate TRPC channels. *J Physiol* 586, 5633-5649.
44. Gopalan SM, Flaim C, Bhatia SN, Hoshijima M, Knoell R, Chien KR, Omens JH, McCulloch AD (2003) Anisotropic stretch-induced hypertrophy in neonatal ventricular myocytes micropatterned on deformable elastomers. *Biotechnol Bioeng* (1(5), 578-587.
45. Gottlieb PA; Bae C, Sachs F (2012) Gating the mechanical channel Piezo1: a comparison between whole-cell and patch recording. *Channels (Austin)* 6, 282-289.
46. Gottlieb PA, Folgering J, Maroto R, Raso A, Wood TG, Kurosky A, Bowman C, Bichet D, Patel A, Sachs F, Martinac B, Hamill OP, Honore E (2008) Revisiting TRPC1 and TRPC6 mechanosensitiviy. *Pflugers Arch* 455(6), 1097-1103.
47. Gottlieb PA, Suchyna TM, Sachs F (2007) Properties and mechanism of the mechanosensitive ion channel inhibitor GsMTx4, a therapeutic peptide derived from tarantula venom. *Curr Top Membr* 59, 81-109.
48. Guinamard R, Chatelier A, Demion M, Potreau D, Patri S, Rahmati M, Bois P (2004) Functional characterization of a Ca(2+)-activated non-selective cation channel in human atrial cardiomyocytes. *J Physiol* 558, 75-83.
49. Gutierrez E, Petrich BG, Shattil SJ, Ginsberg MH, Groisman A, Kasirer-Friede A (2008) Microfluidic devices for studies of shear-dependent platelet adhesion. *Lab Chip* 8(9), 1486-1495.
50. Hamill OP, Marty A, Neher E, Sakmann B, Sigworth FJ (1981) Improved patch-clamp techniques for high-resolution current recording from cells and cell-free membrane patches. *Pflugers Arch* 391(2), 85-100.
51. Harteneck C (2005) Function and pharmacology of TRPM cation channels. *Naunyn Schmiedebergs Arch Pharamcol* 37, 307-314.
52. Heckel E, Boselli F, Roth S, Krudewig A, Belting HG, Charvin G, Vermot J (2015) Oscillatory flow modulates mechanosensitive klf23a expression through trpv4 and trpv2 during heart valve development. *Curr Biol* 25(10), 1354-1361.
53. Heineke J, Ritter O (2012) Cardiomyocyte calcineurin signalling in subcellular domains: from the sarcolemma to the nucleus and beyond. *J Mol Cell Cardiol* 52, 62-73.
54. Higuchi H (1987) Lattice swelling with the selective digestion of elastic components in single-skinned fibers of frog muscle. *Biophys J* 52(1), 29-32.
55. Hill-Eubanks DC, Gonzales AL, Sonkusare SK, Nelson MT (2014) Vascular TRP channels: performing under pressure and going with the flow. *Physiology (Bethesda)* 29(5), 343-360.
56. Hof T, Salle L, Coulbault L, Richer R, Alexandre J, Rouet R, Marique A, Guinamard R (2016) TRPM4 non-selective cation channels influence action potentials in rabbit Purkinje fibres. *J Physiol* 594, 295-306.
57. Hoffman NE, Miller BA, Wang J, Elrod JW, Rajan S, Gao E, Song J, Zhang QX, Hirschler-Laszkiewicz I, Shanmughapriya S, Koch WJ, Feldman AM, Madesh M, Cheung JY (2015) Ca2+ entry via Trpm2 is essential for cardiac myocyte bioenergetics maintenance. *Am J Physiol Heart Physiol* 308, H637-650.
58. Hofmann T, Chubanov V, Gudermann T, Montell C (2003) TRPM5 is a voltage-modulated and Ca2+-activated monovalent selective cation channel. *Curr Biol* 13, 1153-1158.
59. Hofmann T, Obukhov AG, Schaefer M, Harteneck C, Gudermann T, Schultz G (1999) Direct activation of human TRPC6 and TRPC3 channels by diacylglycerol. *Nature* 397, 259-263.
60. Hofmann T, Schaefer M, Schultz G, Gudermann T (2002) Subunit composition of mammalian transient receptor potential channels in living cells. *Proc Natl Acad Sci USA* 99, 7461-7466.
61. Hu L, Ma J, Zhang P, Zheng J (2009) Extracellular hypotonicity induces disturbances of sodium currents in rat ventricular myocytes. *Physiol Res* 58, 807-815.
62. Huang H, Bae C, Sachs F, Suchyna TM (2013) Caveolae regulation of mechanosensitive channel function in myotubes. *PLoS One* 8(8), e72894.

63. Huang L, Li L, Chen X, Zhang H, Shi Z (2016) MiR-103a targeting Piezo1 is involved in acute myocardial infarction through regulating endothelium function. *Cardiol J* 23(5), 556-562.
64. Huang L, Mathieu PS, Helmke BP (2010) A stretching device for high-resolution live-cell imaging. *Ann Biomed Eng* 38(5), 1728-1740.
65. Inoue R, Jensen LJ, Jian Z, Shi J, Hai L, Lurie AI, Henriksen FH, Salomonsson M, Morita H, Kawarabayashi Y, Mori M, Mori Y, Ito Y (2009) Synergistic activation of vascular TRPC6 channel by receptor and mechanical stimulation via phospholipase C/diacylglycerol and phospholipase A2/omega-hydroxylase/20-HETE pathways. *Circ Res* 104, 1399-1409.
66. Inoue R, Jensen LJ, Shi J, Morita H, Nishida M, Nonda A, Ito Y (2006) Transient receptor potential channels in cardiovascular function and disease. *Circ Res* 99(2), 119-131.
67. Inoue R, Okada T, Onoue H, Hara Y, Shimizu S, Naitoh S, Ito Y Mori Y (2001) The transient receptor potential protein homologue TRP6 is the essential component of vascular alpha(1)-adrenoceptor-activated Ca(2+)-permeable cation channel. *Circ Res* 88, 325-332.
68. Iribe G, Kaneko T, Yamaguchi Y, Naruse K (2014) Load dependency in force-length relations in isolated single cardiomyocytes. *Prog Biophys Mol Biol* 115, 103-114.
69. Iribe G, Kohl P (2008) Axial stretch enhances sarcoplasmic reticulum Ca2+ leak and cellular Ca2+ reuptake in guinea pig ventricular myocytes: experiments and models. *Prog Biophys Mol Biol* 97, 298-311.
70. Iribe G, Ward CW, Camelliti P, Bollensdorff C, Mason F, Burton RA, Garny A, Morphew MK, Hoenger A, Lederer WJ, Kohl P (2009) Axial stretch of rat single ventricular cardiomyocytes causes an acute and transient increase in Ca2+ spark rate. *Circ Res* 104(6), 787-795.
71. Ito S, Suki B, Kume H, Namaguchi Y, Ishii M, Iwaki M, Kondo M, Naruse K, Hasegawa Y, Sokabe M (2010) Actin cytoskeleton regulates stretch-activated Ca2+ influx in human pulmonary vascular endothelial cells. *Am J Respir Cell Mol Biol* 43(1), 26-34.
72. Jian Z, Han Z, Zhang T, Puglisi J, Izu LT, Shaw JA, Onofiok E, Erickson JR, Chen YJ, Horvath B, Shimkunas R, Xiao W, Li Y, Pan T, Chan J, Banyasz T, Tardiff JC, Chiamvimonvat N, Bers DM, Lam KS, Chen-Izu Y (2014) Mechanochemotransduction during cardiomyocyte contraction is mediated by localized nitric oxide signaling. *Sci Signal* 7, ra27.
73. Kamaraju K, Gottlieb PA, Sachs F, Sukharev S (2010) Effects of GsMTx4 on bacterial mechanosensitive channels in inside-out patches from giant spheroblasts. *Biophys J* 99(9), 2870-2878.
74. Kamkin A, Kiseleva I, Isenberg G (2003) Activation and inactivation of a non-selective cation conductance by local mechanical deformation of acutely isolated cardiac fibroblasts. *Cardiovasc Res* 57(3), 793-803.
75. Kamkin A, Kiseleva I, Lozinsky I, Scholz H (2005) Electrical interaction of mechanosensitive fibroblasts and myocytes in the heart. *Basic Res Cardiol* 100(4), 337-345.
76. Katanosaka X, Iwasaki K, Ujihara Y, Takatsu S, Nishitsuji K, Kanagawa M, Sudo A, Toda T, Katanosaka K, Mohri S, Naruse K (2014) TRPV2 is critical for the maintenance of cardiac structure and function in mice. *Nat Commun* 5, 3932.
77. Kecskes M, Jacobs G, Kerselaers S, Syam N, Menigoz A, Vangheluwe P, Freichel M, Flockerzi V, Voets T, Vennekens R (2015) The Ca(2+)-activated cation channels TRPM4 is a negative regulator of angiotensin II-induced cardiac hypertrophy. *Basic Res Cardiol* 110, 43.
78. Kim EC, Choi SK, Lim M, Yeon SI, Lee YH (2013) Role of endogenous ENaC and TRP channels in the myogenic response of rat posterior cerebral arteries. *PLoS One* 8, e84194.
79. Kloda A, Martinac B (2002) common evolutionary origins of mechanosensitive ion channels in Archae, Bacteria and cell-walled Eukarya. *Archea* 1, 35-44.
80. Kozera L, White E, Calaghan S (2009) Caveolae act as membrane reserves which limit mechanosensitive I(Cl,swell) channel activation during swelling in the rat ventricular myocyte. *PLoS One* 4(12), e8312.
81. Kreutzer J, Ikonen L, Hirvonen J, Pekkanen-Mattila M, Aalto-Setälä K, Kallio P (2014) Pneumatic cell stretching system for cardiac differentiation and culture. *Med Eng Phys* 36, 396-501.

82. Krueger JW, Young DF, Cholvin NR (1971) An in vitro study of flow response by cells. *J Biomech* 4(1), 31-36.
83. Kuwahara K, Wang Y, McAnally J, Richardson JA, Bassel-Duby R, Hill JA, Olson EN (2006) TRPC6 fulfills a calcineurin signaling circuit during pathologic cardiac remodeling. *J Clin Invest* 116, 3114-3126.
84. Lafaurie-Janvore J, Antoine EE, Perkins SJ, Babataheri A, Barakat AI (2016) A simple microfluidic device to study cell-scale endothelial mechanotransduction. *Biomed Microdevices* 18, 63.
85. Lau OC, Shen B, Wong CO, Tjong YW, Lo CY, Wang HC, Huang Y, Yung WH, Chen YC, Fung ML, Rudd JA, Yao X (2016) TRPC5 channels participate in pressure-sensing in aortic baroreceptors. *Nat Commun* 7, 11947.
86. Le Guennec JY, Peineau N, Argibay JA, Mongo KG, Garnier D (1990) A new method of attachment of isolated mammalian ventricular myocytes for tension recording: length dependence of passive and active tension. *J Mol Cell Cardiol* 22, 1083-1093.
87. Lee JW, Ko YW, Lee IH, Lee HK, Kim HW, Kim YH (2009) Osmotic stress induces loss of glutathione and increases the sensitivity to oxidative stress in H9c2 cardiac myocytes. *Free Radic Res* 43(3), 262-271.
88. Levesque MJ, Nerem RM (1985) The elongation and orientation of cultured endothelial cells in response to shear stress. *J Biomech Eng* 107(4), 341-347.
89. Lewis AH, Grandl J (2015) Mechanical sensitivity of Piezo1 ion channels can be tuned by cellular membrane tension. *eLife* 4, e12088.
90. Li Y, Baylie RL, Tavares MJ, Brayden JE (2014) TRPM4 channels couple purinergic receptor mechanoactivation and myogenic tone development in cerebral parenchymal arterioles. *J Cereb Blood Flow Metab* 34, 1706-1714.
91. Li J, Hou B, Tumova S, Muraki K, Bruns A, Ludlow MJ, Sedo A, Hyman AJ, McKeown L, Young RS, Yuldasheva NY, Majeed Y, Wilson LA, Rode B, Bailey MA, Kim HR, Fu Z, Carter DA, Bilton J, Imrie H, Ajuh P, Dear TN, Cubbon RM, Kearney MT, Prasad KR, Evans PC, Ainscough JF, Beech DJ (2014a) Piezo1 integration of vasculature architecture with physiological force. *Nature* 515, 279-282.
92. Lyons JS, Iyer SR, Lovering RM, Ward CW, Stains JP (2016) Novel multi-functional fluid flow device for studying cellular mechanotransduction. *J Biomech* 49, 4173-4179.
93. Marchenko SM, Sage SO (1997) A novel mechanosensitive cationic channel from the endothelium of rat aorta. *J Physiol* 498, 419-425.
94. Maroto R, Raso A, Wood TG, Kurosky A, Martinac B, Hamill OP (2005) TRPC1 forms the stretch-activated cation channel in vertebrate cells. *Nat Cell Biol* 7(2), 179-185.
95. Martinac B, Adler J, Kung C (1990) Mechanosensitive ion channels of E. coli activated by amphipaths. *Nature* 348, 261-263.
96. Matsumoto T, Delafontaine P, Schnetzer KJ, Tong BC, Nerem RM (1996) Effect of uniaxial, cyclic stretch on the morphology of monocytes/macrophages in culture. *J Biomech Eng* 118(3), 420-422.
97. Matsumoto T, Yung YC, Fischbach C, Kong HJ, Nakaoka R, Mooney DJ (2007) Mechanical strain regulates endothelial cell patterning in vitro. *Tissue Eng* 13(1), 201-217.
98. Mierke CT (2011) Cancer cells regulate biomechanical properties of human microvascular endothelial cells. *J Biol Chem* 286, 40025-40037.
99. Moench I, Meekhof KE, Cheng LF, Lopatin AN (2013) Resolution of hyposmotic stress in isolated mouse ventricular myocytes causes sealing of t-tubules. *Exp Physiol* 98(7), 1164-1177.
100. Mohl MC, Iismaa SE, Xiao XH, Friedrich O, Wagner S, Nikolova-Krstevski V, Wu J, Yu ZY, Feneley M, Fatkin D, Allen DG, Graham RM (2011) Regulation of murine cardiac contractility by activation of α(1A)-adrenergic receptor-operated Ca(2+) entry. *Cardiovasc* Res 91(2), 301-319.
101. Morgan JT, Wood JA, Shah NM, Hughbanks ML, Russel P, Barakat AI, Murphy CJ (2012) Integration of basal topographic cures and apical shear stress in vascular endothelial cells. *Biomaterials* 33(16), 4126-4135.

102. Muraki K Iwata y, Katanosaka Y, Ito T, Ohya S, Shigekawa M, Imaizumi Y (2003) TRPV2 is a component of osmotically sensitive cation channels in murine aortic myocytes. *Circ Res* 93, 829-838.
103. Nakamura K, Koga Y, Sakai H, Homma K, Ikebe M (2007) cGMP-dependent relaxation of smooth muscle is coupled with the change in the phosphorylation of myosin phosphatase. *Circ Res* 101, 712-722.
104. Nakayama H, Wilkin BJ, Bodi I, Molkentin JD (2006) Calcineurin-dependent cardiomyopathy is activated by TRPC in the adult mouse heart. *FASEB J* 20, 1660-1670.
105. Neher E, Sakman B (1976) Single-channel currents recorded from membrane of denervated frog muscle fibres. *Nature* 260, 799-802.
106. Neher E, Sakman B, Steinbach JH (1978) The extracellular patch clamp: a method for resolving currents through individual open channels in biological membranes. *Pflugers Arch* 375, 219-228.
107. Neuman KC, Lionnet T, Allemand JF (2007) Single-molecule micromanipulation techniques. *Annu Rev Mater Res* 37, 33-67.
108. Nikolova-Krstevski V, Wagner S, Yan Yu Z, Cox CD, Cvetkovska J, Hill AP, Huttner IG, Benson V, Werdich A, MacRae C, Feneley MP, Friedrich O, Martinac B, Fatkin D (2017) Endocardial TRPC6 channels act as atrial mechanosensors and load-dependent modulators of endocardial/myocardial cross-talk. *JACC Basic Transl Sci*, **in press**.
109. Nishimura S, Kawai Y, Nakajima T, Hosoya Y, Fujita H, Katoh M, Yamashita H, Nagai R, Sugiura S (2006) Membrane potential of rat ventricular myocytes responds to axial stretch in phase, amplitude and speed-dependent manners. *Cardiovasc Res* 72, 403-411.
110. Nishimura S, Seo K, Nagasaki M, Hosoya Y, Yamashita H, Fujita H, Nagai R, Sugiura S (2008) Responses of single-ventricular myocytes to dynamic axial stretching. *Prog Biophys Mol Biol* 97, 282-297.
111. Nishimura S, Yasuda SI, Kathoh M, Yamada KP, Yamashita H, Saeki Y, Sunagawa K, Nagai R, Hisada T, Sugiura S (2004) Single cell mechanics of rat cardiomyocytes under isometric, unloaded, and physiologically loaded conditions. *Am J Physiol Heart Circ Physiol* 287, H196-H202.
112. Numata T, Shimizu T, Okada Y (2007) Direct mechano-stress sensitivity of TRPM7 channel. *Cell Physiol Biochem* 19, 1-8.
113. Ohba T, Watanabe H, Murakami M, Takahashi Y, Iino K, Kuromitsu S, Mori Y, Ono K, Iijima T, Ito H (2007) Upregulation of TRPC1 in the development of cardiac hypertrophy. *J Mol Cell Cardiol* 42, 498-507.
114. Ohba T, Watanabe H, Takahashi Y, Suzuki T, Miyoshi I, Nakayama S, Satoh E, Iino K, Sasano H, Mori Y, Kuromitsu S, Imagawa K, Saito Y, Iijima T, Ito H, Murakami M (2006) Regulatory role of neuron-restrictive silencing factor in expression of TRPC1. *Biochem Biophys Res Commun* 351, 764-770.
115. Onohara N, Nishida M, Inoue R, Kobayashi H, Sumimoto H, Sato Y, Mori Y, Nagao T, Kurose H (2006) TRPC3 and TRPC6 are essential for angiotensin II-induced cardiac hypertrophy. *EMBO J* 25, 5305-5316.
116. Palmer RE, Brady AJ, Roos KP (1996) Mechanical measurements from isolated cardiac myocytes using a pipette attachment system. *Am J Physiol* 270, C697-C704.
117. Parpaite T, Cardouat G, Mauroux M, Gillibert-Duplantier J, Robilard P, Quignard JF, Marthan R, Savineau JP, Ducret T (2016) Effect of hypoxia on TRPV1 and TRPV4 channels in rat pulmonary arterial smooth muscle cells. *Pflugers Arch* 468, 111-130.
118. Paul NE, Denecke B, Kim BS, Dreser A, Bernhagen J, Pallua N (2017) The effect of mechanical stress on the proliferation, adipogenic differentiation and gene expression of human adipose-derived stem cells. *J Tissue Eng Regen Med*, **in press**.
119. Prosser BL, Khairallah RJ, Ziman AP, Ward CW, Lederer WJ (2013) X-ROS signaling in the heart and skeletal muscle: stretch-dependent local ROS regulates [Ca2+]i. *J Mol Cell Cardiol* 58, 172-181.

120. Prosser BL, Ward CW, Lederer WJ (2011) X-ROS signaling: rapid mechano-chemo transduction in the heart. *Science* 333, 1440-1445.
121. Prosser BL, Ward CW, Lederer WJ (2013a) X-ROS signaling is enhanced and graded by cyclic cardiomyocyte stretch. *Cardiovasc Res* 98(2), 307-314.
122. Qi Y, Li Z, Kong CW, Tang NL, Huang Y, Li RA, Yao X (2015) Uniaxial cyclic stretch stimulates TRPV4 to induce realignment of human embryonic-stem cell-derived cardiomyocytes. *J Mol Cell Cardiol* 87, 65-73.
123. Quick K, Zhao J, Eijkelkamp N, Linley JE, Rugiero F, Cox JJ, Raouf R, Gringhuis M, Sexton JE, Abramowitz J, Taylor R, Forge A, Ashmore J, Kirkwood N, Kros CJ, Richardson GP, Freichel M, Flockerzi V, Birnbaumer L, Wood JN (2012) TRPC3 and TRPC6 are essential for normal mechanotransduction in subsets of sensory neurons and cochlear hair cells. *Open Biol* 2, 120068.
124. Rana OR, Zobel C, Saygili E, Brixius K, Gramley F, Schimpf T, Mischke K, Frechen D, Knackstedt C, Schwinger RHG, Schauerte P, Saygili E (2008) A simple device to apply equibiaxial strain to cells cultured om flexible membranes. *Am J Physiol Heart Circ Physiol* 294, H532-H540.
125. Ranade SS, Qiu Z, Woo SH, Murthy SE, Cahalan SM, Xu J, Mathur J, Bandell M, Coste B, Li YS, Chien S, Patapoutian A (2014) Piezo1, a mechanically activated ion channel, is required for vascular development in mice. *Proc Natl Acad Sci USA* 111, 10347-10352.
126. Randhawa PK, Jaggi AS (2015) TRPV4 channels: physiological and pathophysiological role in cardiovascular system. *Basic Res Cardiol* 110(6), 54.
127. Rapalo G, Herwig JD, Hewitt R, Wilhelm KR, Waters CM, Roan E (2015) Live cell imaging during mechanical stretch. *J Vis Exp* 102, e52737.
128. Reading SA, Brayden JE (2007) Central role of TRPM4 channels in cerebral blood flow regulation. *Stroke* 38, 2322-2328.
129. Retailleau K, Duprat F, Arhatte M, Ranade SS, Peyronnet R, Martins JR, Jodar M, Moro C, Offermanns S, Feng Y, Demolombe S, Patel A, Nonore E (2015) Piezo1 in smooth muscle cells is involved in hypertension-dependent arterial remodeling. *Cell Rep* 13(6), 1161-1171.
130. Ridone P, Nakayama Y, Martinac B, Battle AR (2015) Patch clamp characterization of the effect of cardiolipin on MscS of *E.coli*. *Eur Biophys J* 44(7), 567-577.
131. Riemer TL, Tung L (2003) Stretch-induced excitation and action potential changes of single cardiac cells. *Prog Biophys Mol Biol* 82, 97-110.
132. Rutkowskiy A, Nliksoen M, Hilletstad V, Amin M, Czibik G, Valen G, Vaage J, Amiry-Moghaddam M, Stenslokken KO (2013) Aquapirin-1 in cardiac endothelial cells is downregulated in ischemia, hypoxia and cardioplegia. *J Mol Cell Cardiol* 56, 22-33.
133. Rutkowskiy A, Valen G, Vaage J (2013a) Cardiac aquaporins. *Basic Res Cardiol* 108(6), 393.
134. Sadoshima JI, Takahashi T, Jahn L, Izumo S (1992) Roles of mechano-sensitive ion channels, cytoskeleton, and contractile activity in stretch-induced immediate-early gene expression and hypertrophy of cardiac myocytes. *Proc Natl Acad Sci USA* 89, 9905-9909.
135. Sah R, Mesirca P, Mason X, Gibson W, Bates-Withers C, Van den Boogert M, Chaudhuri D, Pu WT, Mangoni ME, Clapham DE (2013) Timing of myocardial trpm7 deletion during cardiogenesis variably disrupts adult ventricular function, conduction and repolarization. *Circulation* 128, 101-114.
136. Sah R, Mesirca, Van den Boogert M, Rosen J, Mably J, Mangoni ME, Clapham DE (2013a) Ion channel-kinase TRPM7 is required for maintaining cardiac automaticity. *Proc Natl Acad Sci USA* 110, E3037-E3046.
137. Saitou T, Ishikawa T, Obara K, Nakayama K (2000) Characterization of whole-cell currents elicited by mechanical stimulation of *Xenopus* oocytes. *Pflugers Arch* 440, 858-865.
138. Samuel JL, Vandenburgh HH (1990) Mechanically induced orientation of adult rat cardiac myocytes in vitro. *In Vitro Cell Dev Biol* 26, 905-914.
139. Sasaki N, Mitsuiye T, Noma A (1992) Effects of mechanical stretch on membrane currents of single ventricular myocytes of guinea-pig heart. *Jpn J Physiol* 42(6), 957-970.

140. Satoh T, Narazaki G, Sugita R, Kobayashi H, Sugiura S, Kanamori T (2016) A pneumatic pressure-driven multi-throughput microfluidic circulation culture system. *Lab Chip* 16, 2339.
141. Schürmann S, Wagner S, Herlitze S, Fischer C, Gumbrecht S, Wirth-Hücking A, Prölß G, Lautscham LA, Fabry B, Goldmann WH, Nikolova-Krstevski V, Martinac B, Friedrich O (2016) The IsoStretcher: an isotropic cell stretch device to study mechanical biosensor pathways in living cells. *Biosens Bioelectron* 81, 363-372.
142. Seth M, Zhang ZS, Mao L, Graham V, Burch J, Stiber J, Tsiokas L, Winn M, Abramowitz J, Rockman HA, Birnbaumer L, Rosenberg P (2009) TRPC1 channels are critical for hypertrophic signaling in the heart. *Circ Res* 105(10), 1023-1030.
143. Shan D, Marchase RB, Chatham JC (2008) Overexpression of TRPC3 increases apoptosis but not necrosis in response to ischemia-reperfusion in adult mouse cardiomyocytes. *Am J Physiol Cell Physiol* 294, C833-C841.
144. Shen B, Wong CO, Lau OC, Woo T, Bai S, Huang Y, Yao X (2015) Plasma membrane mechanical stress activates TRPC5 channels. *PLoS One* 10(4), e0122227.
145. Shenton FC, Pyner S (2014) Expression of transient receptor potential channels TRPC1 and TRPV4 in venoatrial endocardium of the rat heart. *Neuroscience* 267, 195-204.
146. Shi Y, Dong Y, Duan Y, Jiang X, Chen C, Deng L (2013) Substrate stiffness influences TGF-ß1-induced differentiation of bronchial fibroblasts into myofibroblasts in airway remodelling. *Mol Med Rep* 7(2), 419-424.
147. Song S, Yamamura A, Yamamura H, Ayon RJ, Smith KA, Tang H, Makino A, Yuan JX (2014) Flow shear stress enhances intracellular Ca2+ signaling in pulmonary artery smooth muscle cells from patients with pulmonary arterial hypertension. *Am J Physiol Cell Physiol* 307, C373-C383.
148. Sonkusare SK, Bonev AD, Ledoux J, Liedtke W, Kotlikoff MI, Heppner TJ, Hill-Eubanks DC, Nelson MT (2012) Elementary Ca2+ signals through endothelial TRPV4 channels regulate vascular function. *Science* 336, 597-601.
149. Spassova MA, Hewavitharama T, Xu W, Soboloff J, Gill DL (2006) A common mechanism underlies stretch activation and receptor activation of TRCP6 channels. *Proc Natl Acad USA* 103, 16586-16591.
150. Strubing C, Krapivinsky G, Krapivinsky L, Clapham DE (2001) TRPC1 and TRPC5 form a novel cation channel in mammalian brain. *Neuron* 29, 645-655.
151. Sullivan MN, Earley S (2013) TRP channel Ca^{2+} sparklets: fundamental signals underlying endothelium-dependent hyperpolarization. *Am J Physiol Cell Physiol* 305, C999-C1008.
152. Sun YH, Li YQ, Feng SL, Li BX, Pan ZW, Xu CQ, Li TT, Yang BF (2010) Calcium-sensing receptor activation contributed to apoptosis stimulates TRPC6 channel in rat neonatal ventricular myocytes. *Biochem Biophys Res Commun* 394, 955-961.
153. Swaminathan V, Mythreye K, O'Brien ET, Berchuck A, Blobe GC, Superfine R (2011) Mechanical stiffness grades metastatic potential in patient tumor cells and cancer cell lines. *Cancer Res* 71(15), 5075-5080.
154. Syeda R, Florendo MN, Cox CD, Kefauver JM, Santos JS, Martinac B, Patapoutian A (2016) Piezo1 channels are inherently mechanosensitive. *Cell Rep* 17, 1739-1746.
155. Takeuchi A, Tatsumi S, Sarai N, Terashima K, Matsuoko S, Noma A (2006) Ionic mechanisms of cardiac cell swelling induced by blocking Na+/K+ pump as revealed by experiments and simulation. *J Gen Physiol* 128(5), 495-507.
156. Tan W, Scott D, Belchenko D, Qui HJ, Xiao L (2008) Development and evaluation of microdevices for studying anisotropic biaxial stretch on cells. *Biomed Microdevices* 10(6), 869-882
157. Tang C, To WK, Meng F, Wang Y, Gu Y (2010) A role for receptor-operated Ca2+ entry in human pulmonary artery smooth muscle cells in response to hypoxia. *Physiol Res* 59(6), 909-918.
158. Teng J, Loukin S, Anishkin A, Kung C (2015) The force-from-lipid (FFL) principle of mechanosensitivity, at large and in elements. *Pflügers Arch* 467, 27-37.
159. Thodeti CK, Paruchuri S, Meszaros JG (2013) A TRP to cardiac fibroblast differentiation. *Channels (Austin)* 7, 211-214.

160. Thompson SA, Copeland CR, Deich DH, Tung L (2011) Mechanical coupling between myofibroblasts and cardiomyocytes slows electrical conduction in fibrotic cell monolayers. *Circulation* 123, 2083-2093.
161. Tung L, Zou S (1995) Influence of stretch on excitation threshold of single from ventricular cells. *Exp Physiol* 80, 221-235.
162. Ueki Y, Sakamoto N, Sato M (2010) Cyclic force applied to FAs induces actin recruitment depending on the dynamic loading pattern. *Open Biomed Eng J* 4, 129-134.
163. Vandenburg JI, Yoshida A, Kirk K, Powell T (1994) Swelling-activated and isoprenaline-activated chloride currents in guinea pig cardiac myocytes have distinct electrophysiology and pharmacology. *J Gen Physiol* 104, 997-1017.
164. Vandenburgh HH (1988) A computerized mechanical cell stimulator for tissue culture: effects on skeletal muscle organogenesis. *In Vitro Cell Dev Biol* 24(7), 609-619.
165. Vandenburgh HH, Karlisch P (1989) Longitudinal growth of skeletal myotubes in vitro in a new horizontal mechanical cell stimulator. *In Vitro Cell Dev Biol* 25(7), 607-616.
166. Vandenburgh HH, Kaufman S (1979) In vitro model for stretch-induced hypertrophy of skeletal muscle. *Science* 203, 265-268.
167. Wang D, Xie Y, Yuan B, Xu J, Gong P, Jiang X (2010) A stretching device for imaging real-time molecular dynamics of live cells adhering to elastic membranes on inverted microscopes during the entire process of the stretch. *Integr Biol* 2, 288-293.
168. Wang J, May Y, Sachs F, Li J, Suchyna TM (2016) GsMTx4-D is a cardioprotectant against myocardial infarction during ischemia and reperfusion. *J Mol Cell Cardiol* 98, 83-94.
169. Wang S, Chenupati R, Kaur H, Iring A, Wettschureck N, Offermanns S (2016a) Endothelial cation channel Piezo1 controls blood pressure by mediating flow-induced ATP release. *J Clin Invest* 126, 4527-4536.
170. Wang Y, Xiong Z, Gong W, Zhou P, Xie Q, Zhou Z, Lu G (2013) Expression of heat shock protein 27 correlates with actin cytoskeletal dynamics and contractility of cultured human bladder smooth muscle cells. *Exp Cell Res* 338(1), 39-44.
171. Watanabe H, Murakami M, Ohba T, Takahashi Y, Ito H (2008) TRP channel and cardiovascular disease. *Pharmacol Ther* 118, 337-351.
172. Wilson C, Dryer SE (2014) A mutation in TRPC6 channels abolishes their activation by hypoosmotic stretch but does not affect activation by diacyglycerol of G protein signaling cascades. *Am J Physiol Renal Physiol* 306(9), F1018-F1025.
173. Wu X, Eder P, Chang B, Molkentin JD (2010) TRPC channels are necessary mediators of pathologic cardiac hypertrophy. *Proc Natl Acad Sci USA* 107, 7000-7005.
174. Yamamoto K, Dang QN, Kelly RA, Lee RT (1998) Mechanical strain suppresses inducible nitric-oxide synthase in cardiac myocytes. *J Biol Chem* 273(19), 11862-11866.
175. Yang KT, Chang WL, Yang PC, Chien CL, Lai MS, Su MJ, Wu ML (2006) Activation of the transient receptor potential M2 channel and poly(ADP-ribose) polymerase is involved in oxidative stress-induced cardiomyocyte death. *Cell Death Differ* 13, 1815-1826.
176. Yang XR, Lin AH, Hughes JM, Flavahan NA, Cao YN, Liedtke W, Sham JS (2012) Upregulation of osmo-mechanosensitive TRPV4 channels facilitates chronic hypoxia-induced myogenic tone and pulmonary hypertension. *Am J Physiol Lung Cell Mol Physiol* 302, L555-L568.
177. Yasuda SI, Sugiura S, Kobayakawa N, Fujita H, Yamashita H, Katoh K, Saekl Y, Kaneko H, Suda Y, Nagai R, Sugi H (2001) A novel method to study contraction characteristics of a single cardiomyocyte using carbon fibers. *Am J Physiol Heart Circ Physiol* 281, H1442-H1446.
178. Yeves AM, Villa-Abrille MC, Perez NG, Medina AJ, Escudero EM, Ennis IL (2014) Physiological cardiac hypertrophy: critical role of AKT in the prevention of NHE-1 hyperactivity. *J Mol Cell Cardiol* 76, 186-195.
179. Yin J, Kuebler WM (2010) Mechanotransduction by TRP channels: general concepts and specific role in the vasculature. *Cell Biochem Biophys* 56, 1-18.

180. Yoshida T, Inoue R, Morii T, Takahashi N, Yamamoto S, Hara Y, Tominaga M, Shimuzu S, Sato Y, Mori Y (2006) Nitric oxide activates TRP channels by cysteine S-nitrosylation. *Nat Chem Biol* 2, 596-607.
181. Yost MJ, Simpson D, Wrona K, Ridley S, Ploehn HJ, Borg TK, Terracio L (2000) Design and construction of a uniaxial cell stretcher. *Am J Physiol Heart Circ Physiol* 279, H3124-H3130.
182. Yue Z, Xie J, Yu AS, Stock J, Du J, Yue L (2015) Role of TRP channels in the cardiovascular system. *Am J Physiol Heart Circ Physiol* 308, H157-H182.
183. Zeng T, Bett GCL, Sachs F (2000) Stretch-activated whole cell currents in adult rat cardiac myocytes. *Am J Physiol Heart Circ Physiol* 278, H548-H557.
184. Zhang DX, Guttermann DD (2012) Transient receptor potential channel activation and endothelium-dependent dilation in the systemic circulation. *J Cardiovasc Pharmacol* 57, 133-139.
185. Zhang X, Huk DJ, Lincoln J, Zhao Y (2014) A microfluidic shear device that accommodates parallel high and low stress zones within the same culturing chamber. *Biomicrofluidics* 8, 054106.
186. Zhang Y, Li TS, Lee ST, Wawrowsky KA, Cheng K, Galang G, Malliaras K, Abraham MR, Wang C, Marban E (2010) Dedifferentiation and proliferation of mammalian cardiomyocytes. *PLoS One* 5(9), e12559.
187. Zhou J, Khokadov DA, Ellis AV, Voelcker NH (2012) Surface modifications for PDMS-based microfluidic devices. *Electrophoresis* 3(1), 89-104.
188. Ziemann F, Rädler J, Sackmann E (1994) Local measurements of viscoelastic moduli of entangled actin networks using an oscillating magnetic bead microrheometer. *Biophys J* 66, 2210-2226.

Methods

IsoStretcher experiments involving 3D hydrogel-embedded adult cardiomyocytes (Fig. 5B)

Chamber preparation. The stretcher chambers, as described by Schürmann et al. (2016), are stored in 70 % ethanol while not in use. Before use, the chambers are additionally sterilized by exposure to UV-Light for at least 20 min, then filled with laminin solution (20 µg/µl, Gibco) to cover the bottom (in our case ~100 µl) and incubated overnight. Before embedding cells on the chambers, the laminin solution is removed and the chamber is dried to avoid diluting the embedding gel.

Embedding of Cardiomyoctes. Ventricular mouse CM were obtained by a standard Langendorff isolation according to Mohl et al. (2011) with a sedimentation separation follow-up step. The cardiomyocytes are kept in ADS buffer until embedding (max. 1 h). To form the embedding hydrogel, the PVA-PEG Hydrogel SG Kit from *Cellendes* was used (Cellendes GmbH, Reutlingen, Germany). Additionally, 3D Life RGD Peptide (Cellendes) was incorporated into the gel to facilitate cell adhesion to the hydrogel. A precursor solution is formed by mixing the RGD peptide solution with the main gel components, except for the cells and the gel cross-linking component (see Table 1). The precursor is incubated for 20 min at RT to anneal RGD peptides to PVA molecules. After incubation, the cells and PEG-linker are added and swiftly mixed. Fluo-4 AM (10 µM, Molecular Probes) was added at the same time as the cells and cross-linker. Depending on the desired gel strength (see Table 1), the mixture had to be plated onto the chambers quickly. Gel mixtures composed after the 'strong' recipe can no longer be handled by pipette about 3 min after adding the PEG-Link, the time window becomes increasingly larger when using recipes for less concentrated gel mixtures. Either 30 µl or 15 µl of gel mixture were plated on each chamber. The resulting cardiomyocyte count per chamber was about 10,000. After plating, the gel mixture was incubated until a firm gel was formed ('weak' ~70 min, 'medium' ~25 min, 'strong' ~10 min). The stiffness of the gels was experimentally determined using a commercial nanoindenter system (Piuma Nanoindenter, Optics 11, Amsterdam, Netherlands), indenting the gel with a stiff cantilever at given force and measuring the indentation by displacement of the cantilever using laser interferometry. We obtained values of ~1 kPa for the weak gel, 4-9 kPa for the

medium gel and >10 kPa for the strong gel as Young modulus. Before experiments, the gel was covered with Tyrode solution additionally containing 20 mM HEPES and with a reduced calcium content of 0.4 µM (~150 µl). Culture medium was exchanged after 1 h to remove remnants of gel monomers and buffer.

Live-cell confocal imaging. Cells were imaged though the bottom of the PDMS chambers mounted in the *Isostretcher* on a confocal fluorescence microscope (Zeiss LSM 750, Zeiss, Melbourne, Australia). The chambers were mounted in a relaxed position and stretched in hardware stretch steps of 5 % while adjusting for eventual focus shifts recording images after each stretch step. The applied stretching speed was 20 % s^{-1} rendering each 5 % step completed at roughly 0.25 s. Stretching experiments were done within 4 h after the embedding, as culturing the cells overnight has not shown to improve cell-gel adhesion but did increase cell mortality. Image analysis was performed with *ImageJ* software package. The fluorescence image of a cell was normalized and a threshold of 15 % maximum intensity was applied to eliminate background noise. To estimate the cell boundaries, the Analyze Particles plugin was used. The plugin returns a boundary line as well as well as the calculated cross section area size in µm². The actual cell stretch is determined by observing the increase of cross section area.

***IsoStretcher* experiments involving HEK293 cells (Fig. 7A)**

About 15,000 HEK293 cells were seeded directly to the central reservoir of the PDMS chamber (final volume ~100 µl. Adhesion of cells was allowed overnight. The mCherry Piezo1 construct has been previously characterized and the channel behavior is similar to wild type Piezo1 (Cox et al. 2016). Before transfecting HEK293 cells with Piezo1 construct using Lipofectamine 3000 Transfection Reagent (Thermo Fisher Scientific), they were washed once with warm PBS. The next day, cells were washed and stained in Ca^{2+} free solution with Fluo-4 AM (10 µM, Molecular Probes) for 15 min at 37 ℃. Before the experiments, cells were washed with warm PBS three times. The *IsoStretcher* was operated at a speed of 20 % s^{-1}. The initial stretch was applied to the sample 1 % at a time up to 20 % while controlling focus. Following the peak of stretch-induced intracellular Ca^{2+} fluorescence intensity, the sample was relaxed back to 0 % and re-stretched again to 20 % hardware stretch without

intermittent steps at a speed of 20 % s^{-1}. After another 20 s of recording, the substrate was relaxed back to 0 % hardware stretch.

Tables

Table 1: Hydrogel recipes for low, medium and high concentration of thiol groups in gels, resulting in 'weak', 'medium' and 'strong' gels. The thiol group concentrations in each of the gels are: 2 mM, 5 mM and 9 mM, respectively, resulting in an elastic modulus of ~1 kPa, 4-9 kPa and >10 KPa. Components of the precursor solution are highlighted in grey. The components not highlighted were added after the precursor mix was incubated for 20 min at RT. The gel starts forming after addition of the PEG-Link cross-linker and is solid enough to be covered in culture medium after 70, 25 and 10 minutes for low, medium and high concentration gels. The recipes were derived from the original recipes provided alongside the Hydrogel Kit by Cellendes.

Component for 31.1 µl gel	Low ('weak')	Medium ('medium')	High ('strong')	Volume unit
water	17.5	10	0	µl
1ßx CB buffer	2.5	2.5	2.5	
SG-PVA	2	5	9	
RGD Peptide	0.8	0.8	0.8	
Fluo-4 AM	0.3	0.3	0.3	
Cell suspension	5	5	5	
PEG-linker	3	7.5	13.5	

Figure Legends

Figure 1: Integrated overview of the involvement of mechanosensitive channels, in particular the TRP and Piezo-family in the cardiovascular system. Both in heart and vasculature, the principal lining of interacting cell types is given by muscle cells (cardiomyocytes, CM, vascular smooth muscle cells, VSMC), fibroblasts and endothelial cell (EC). Although not all TRP channel family members have been determined as 'mechanosensitive'; they all conduct cations, i.e. Ca^{2+} and Na^{+} at varying relative selectivity. In EC, mechanosensitive channels are mostly employed in conveying vasodilative effects, i.e. through NO production and membrane hyperpolarization directly conducted to adjacent VSMC via myoendothelial coupling (gap junctions). In VSMC, effects from neighboring EC mostly activate myosin-light chain phosphatase (MLCP), favoring muscle relaxation. Direct VSMC mechanical stimulation activates intrinsic TRPC members to induce Ca^{2+} influx, membrane depolarization and subsequent myosin-light chain kinase activation and thus, vasoconstriction. In CM, receptor-operated TRP activation is a predominant mechanism over direct mechanical stimulation for most TRP family members and may be additive to those who are inherently mechanosensitive. TRP channels in fibroblasts are mostly associated with hypertrophy and fibrosis responses. For details, see text. ENaC: epithelial Na^{+} channel. eNOS: epithelial NO-synthase. VGCC: voltage-gated Ca^{2+} channel. cGMP: cyclic guanosyl-monophosphate. BK_{Ca}: Ca^{2+}-regulated K^{+}-channel of large conductance. (p)AKT: (phosphorylated) AKT. PI3K: phosphatidyl-inositol-3-kinase. PA: pulmonary artery. CV: central vein. LV/RV: left/right ventricle. AT-II: angiotensin-II. ET-1: endothelin-1. NFAT: nuclear factor of activated transcription. ROS: reactive oxygen species. Cyt C: cytochrome C. DAG: diacylglycerol. PIP2: Phosphatidyl-inositol-diphosphate. IP3: inositol-3-phosphate. RYR2: ryanodine receptor 2. GPCR: G-protein coupled receptor

Figure 2: Local mechanical membrane stimulation and osmotic manipulations of membrane strain. A, pipette-suction-induced membrane stretch to study MSC activity in patch clamp settings using cell-attached single channel, inside-out or outside-out patch clamp configurations. Suction can be applied to mechanically bend the membrane and to activate MSC within the patch areal (data shown from

Sadoshima et al. 1992). **B,** hypoosmotic shock in cells is usually employed by lowering osmolarity of the bathing solution. Due to osmotic gradients, water influx into the cells occurs. Activation of MSC can be monitored by simultaneous electrophysiology. For details, see text (data shown from Clemo et al. 1998). **C,** shear-flow-induced lateral mechanical stress to cell membranes by microfluidics systems (pipette-based jet-injection of microfluidic chambers involving pump systems). For details see text. **D,** local manual indentation of membrane by stamp-press devices and micromanipulator actuation systems. For details, see text. **E,** magnetic tweezer technology to apply localized tethered membrane pinch to ECM-protein coated micro-beads and applying an external magnetic field. For details, see text.

Figure 3: Axial stretch technologies for elongated cells (i.e. cardiomyocytes) using mechanical fixation to stiff supports. A, carbon rods, either bare or coated with bio-adhesive polymers, point-attach CM near both ends by touching the CM membrane perpendicularly to the main axis. Upon contact, CM firmly attach to the carbon fibre rods and even support submaximal isometric contractions. With micromanipulators attached to the rods, defined stretches can be applied. Electrophysiology can additionally be established by positioning a microelectrode distally to the stationary carbon rod, while the opposite rod is used to stretch the cell (photograph and data from Belus & White 2003). **B,** glass-pipette approach using coarse fire-polished glass pipettes with larger diameter compared to patch pipettes to approach elongated cells (i.e. CM) from both ends and either sucking in the distal portion of the membrane or applying adhesives. Several designs from single- or double-barreled pipettes have been developed. Usually, one pipette remains stationary while the opposite is retracted by micro-actuators. Electrophysiology pipettes can additionally be employed in between. For details see text (photographs and data from Zeng et al. 1996).

Figure 4: Elastomer substrate-based stretch technologies with pneumatic or mechanical (uniaxial) actuation. A, pneumatically actuated membrane systems as developed and distributed e.g. by *FlexCell® Int.* using either spherical bulging of an elastomer membrane or directed uniaxial stretch by introducing loading posts

underneath the elastomer. In either case, optical visualization is hampered by marked z-shifts during membrane bulging or blocking loading posts. Another design by Kreutzer et al. (2014) (right panel) employs pneumatic suction introduced between PDMS cast walls to buckle the thin elastomer membrane bottom to which cells are adhered. Again, z-focus drifts are in the range of 350 µm for 10 % stretch. **B,** mechanical uniaxial stretch systems using stepper motor actuation to stretch silastic membrane patches clamped to a static post and the motor arm. Uniaxial stretch experiments can employ cyclic or static stretch protocols. Designs involving supporting base plates usually prevent inverted microscopy of cells and only allow post-stretch visualization in then fixed cells. Dynamic stretch is very potent in repatterning adhered cells. Mostly, endothelia, epithelial or neonatal CM are used in the literature as these cells stick readily and strongly to ECM-coated elastomer membranes (photographs from Matsumoto et al. 2007). For details see text.

Figure 5: Model of uniaxial versus isotropic stretch employing isolated cells or cells within tissue and suggested loop of mechanical biosensor-bioactuator signaling in cells. A, in the literature, stretch of cells adhered in 2D elastomeric substrates is usually performed. In particular in elongated CMs with two perpendicular membrane systems (sarcolemma and tubules), uniaxial stretch is supposed to stretch the sarcolemma and slacken the tubules. Multiaxial stretch represents a more physiological stretch regime where organ wall tension is transduced onto both membrane systems. *Cell-in-a-gel* isotropic stretch with embedded RGD peptide sequences is preferable over 2D coatings and probably the only feasible stretch solution for adult CM which require FAC-anchorage to ECM proteins. In EC, uniaxial versus isotropic stretch results in different stretch-induced responses with reorientation of cells under uniaxial stretch. **B,** suggested stretch-sensing and cellular actuation loop involving membrane stretch sensors, such as mechanosensitive TRP channels that answer membrane stretch by Ca^{2+} influx. The latter is supposed to trigger multiple, yet poorly identified, signaling pathways that lead to upregulation of focal adhesion complex proteins, thus repatterning ECM anchorage. We hypothesize that stronger mechanical stretch is answered by tighter embedding and repatterning of cells within the extracellular matrix.

Figure 6: Mechanically actuated elastomer substrate-based stretch technologies for multiaxial/isotropic cell stretch. A, mechanically actuated system involving vertical displacement of a membrane holder ring over a bottom-fixed indenter ring of variable shape to apply uniaxial or isotropic stretch to the elastomer substrate, as verified by fluorescent bead tracking. Using that system on HUVEC cells, a larger number and extension of FAC points was verified for isotropic stretch over uniaxial stretch (data from Huang et al. 2010). **B,** recently engineered *IsoStretcher* system employing a rotational-to-radial translation of pins moving within a radial guidance groove via a translation ring with oblique trenches. The system is suitable for live-cell fluorescence microscopy **(i)**. Isotropicity was verified with fluorescent beads **(ii)**. **(iii)** Stretch transmission from the substrate membrane to cell membrane area was explicitly verified to validate stretch amplitudes up to which cell membrane stretch can be linearly followed (data from Schürmann et al. 2016).

Figure 7: Isotropic stretch of HEK293 cells and 3D embedded *cell-in-a-gel* adult ventricular cardiomyocytes using the *IsoStretcher* system. A, Piezo1-expressing HEK293 cells stained with Fluo-4 were statically stretched to 20 % and intracellular Ca^{2+} fluorescence monitored. Stretch was answered by a fast increase in $[Ca^{2+}]_i$ that slowly inactivated during maintained stretch and declined faster upon unstretching, demonstrating mechanosensitivity of Piezo1 over control HEK cells (not shown). **B, (i)** adult ventricular mouse CM imaged along the trajectory of isotropic stretch from 0 % to 15 % 3D-embedded in a PVA hydrogel with 9 mM thiol concentration ('strong Gel'). Cell surface increases in both lateral and longitudinal direction. **(ii)** group analysis from several gels shows that weak gels are too compliant to translate substrate elastomer stretch to the cell membrane. The stiffer the gel, the better the translation of mechanical stretch to cells. **(iii)** first results on single CM embedded in a PVA-hydrogel stretching to 19 % and stained with Fluo-4. A prominent increase in Ca^{2+}-fluorescence can be detected with an amplitude of approx. 5 % over baseline in a normal wt cardiomyocyte.

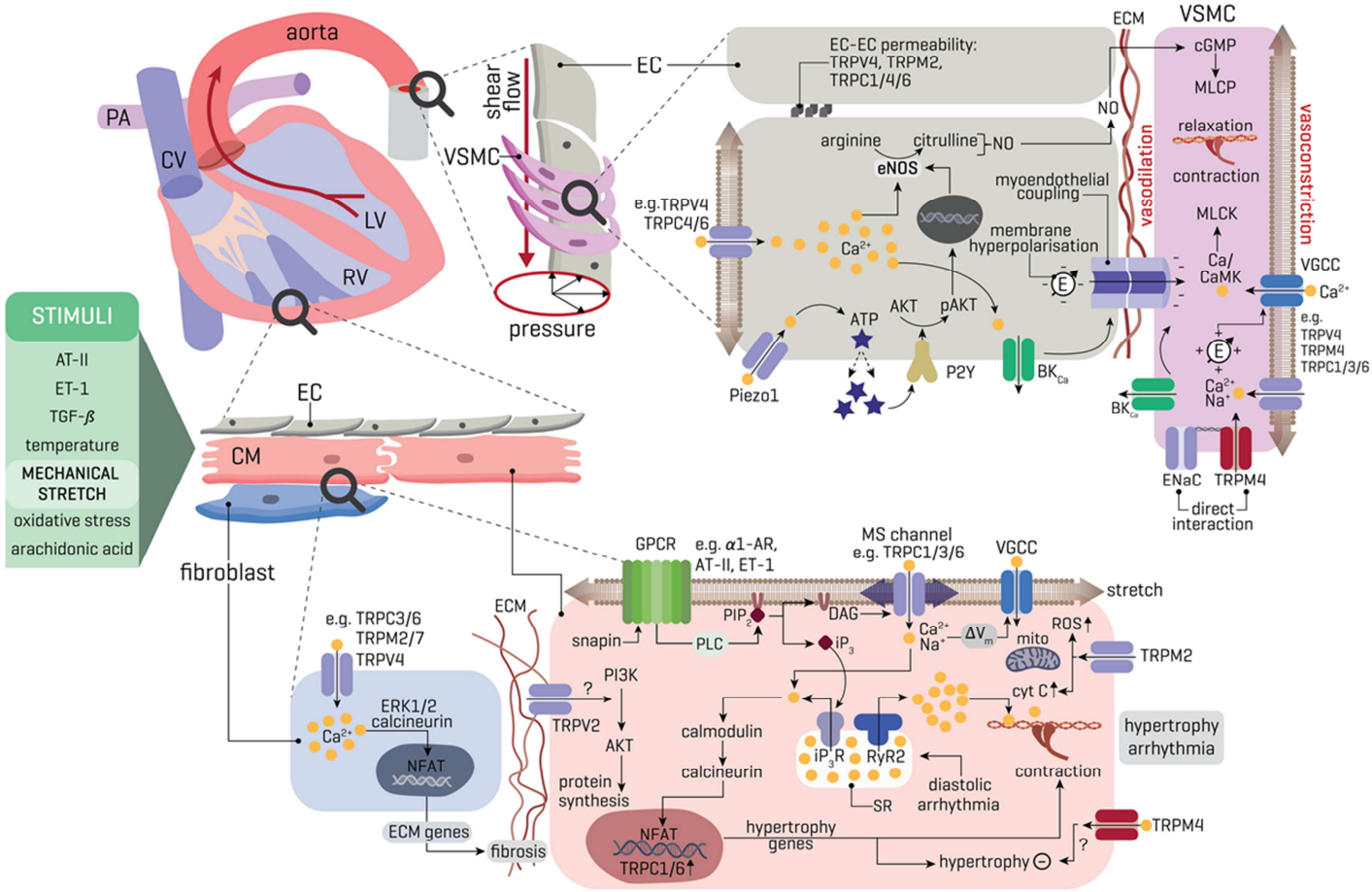

Figure 1 (Friedrich et al. 2017)

1830

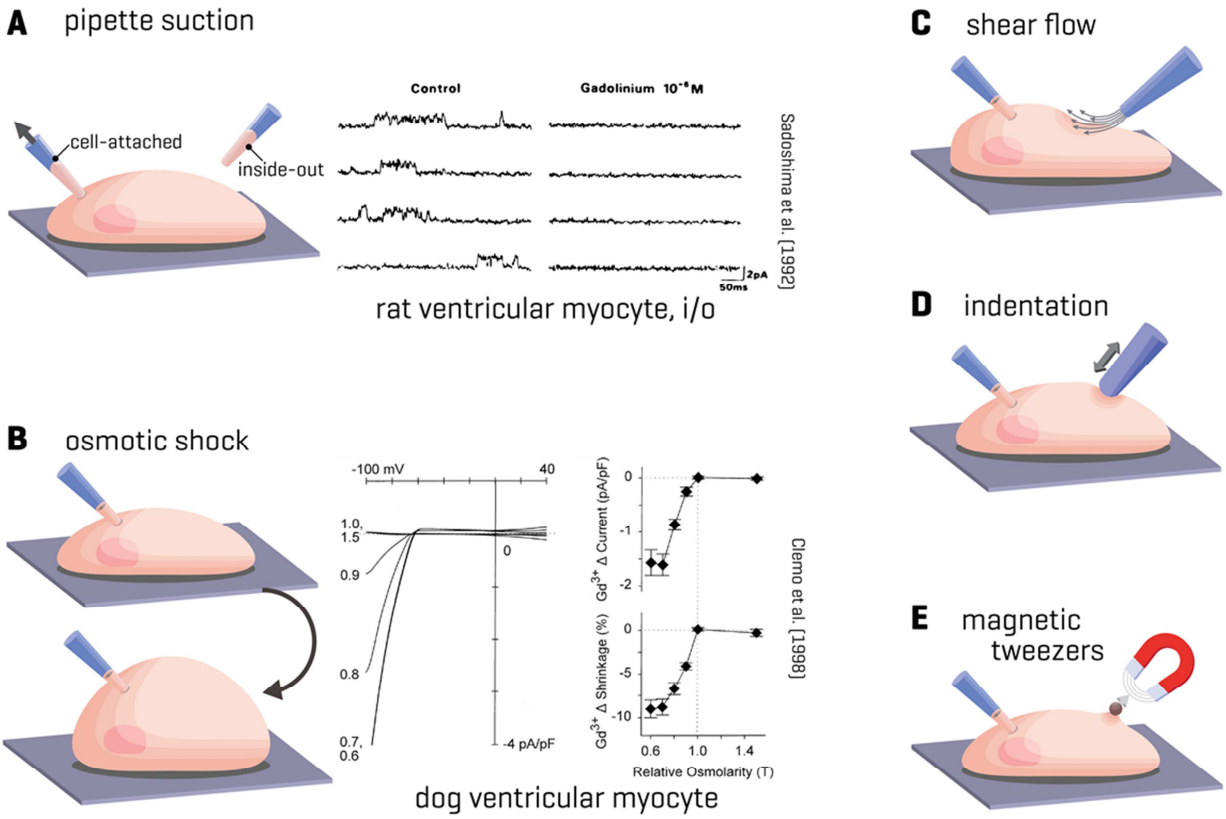

1831

1832

1833 **Figure 2 (Friedrich et al. 2017)**

1834

1835

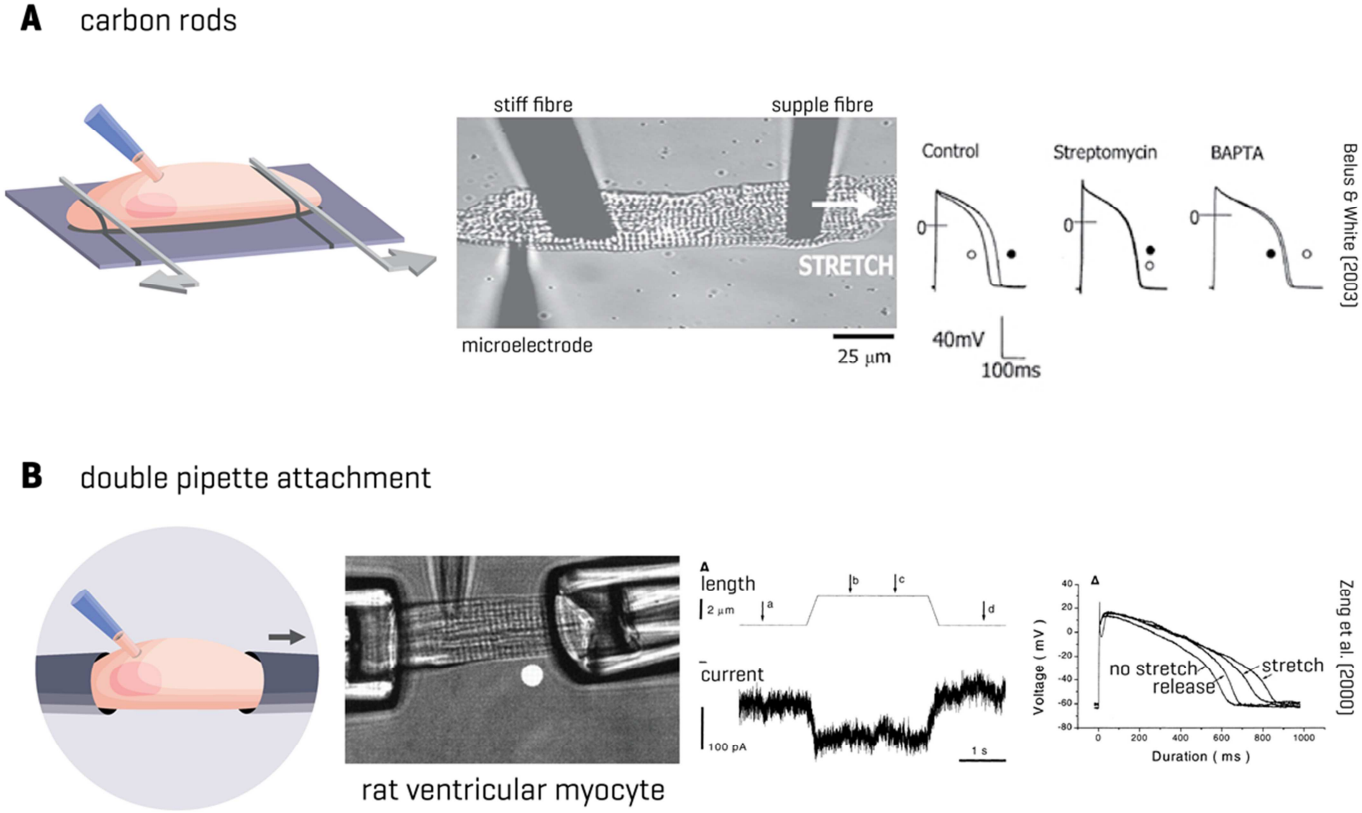

1...

1837

1838 **Figure 3 (Friedrich et al. 2017)**

1839

1840

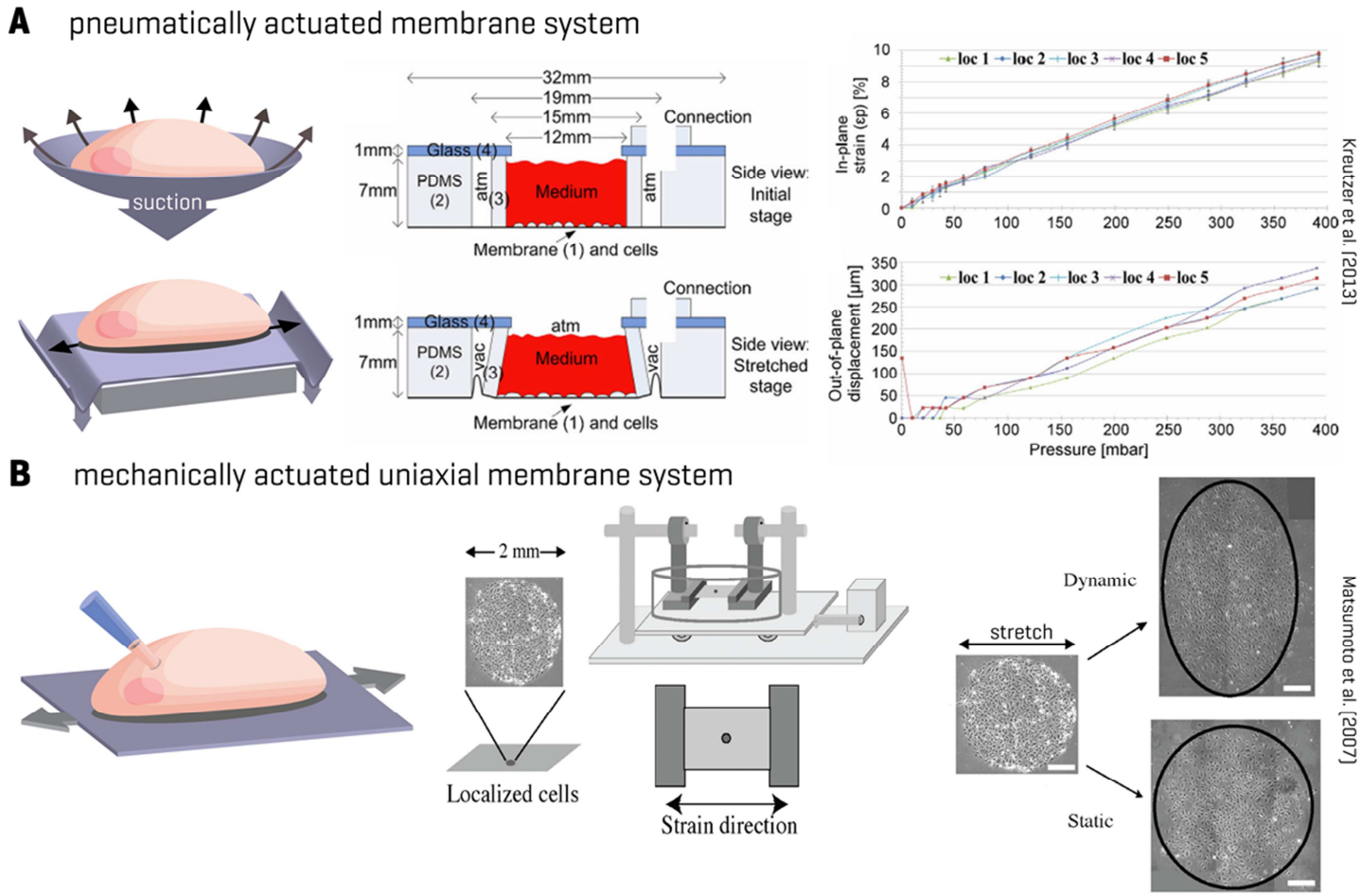

Figure 4 (Friedrich et al. 2017)

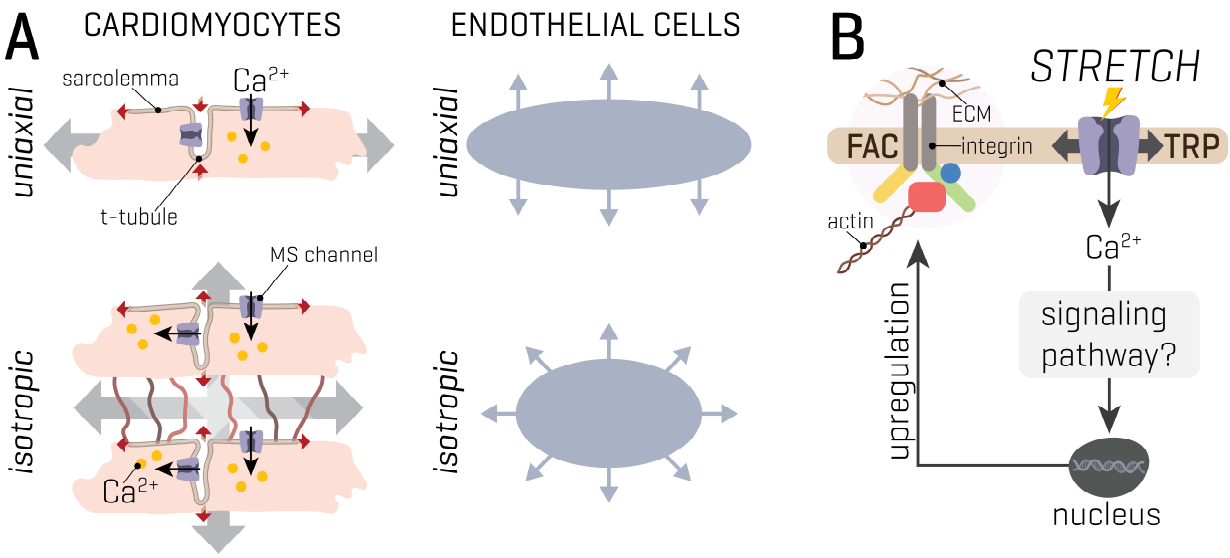

Figure 5 (Friedrich et al. 2017)

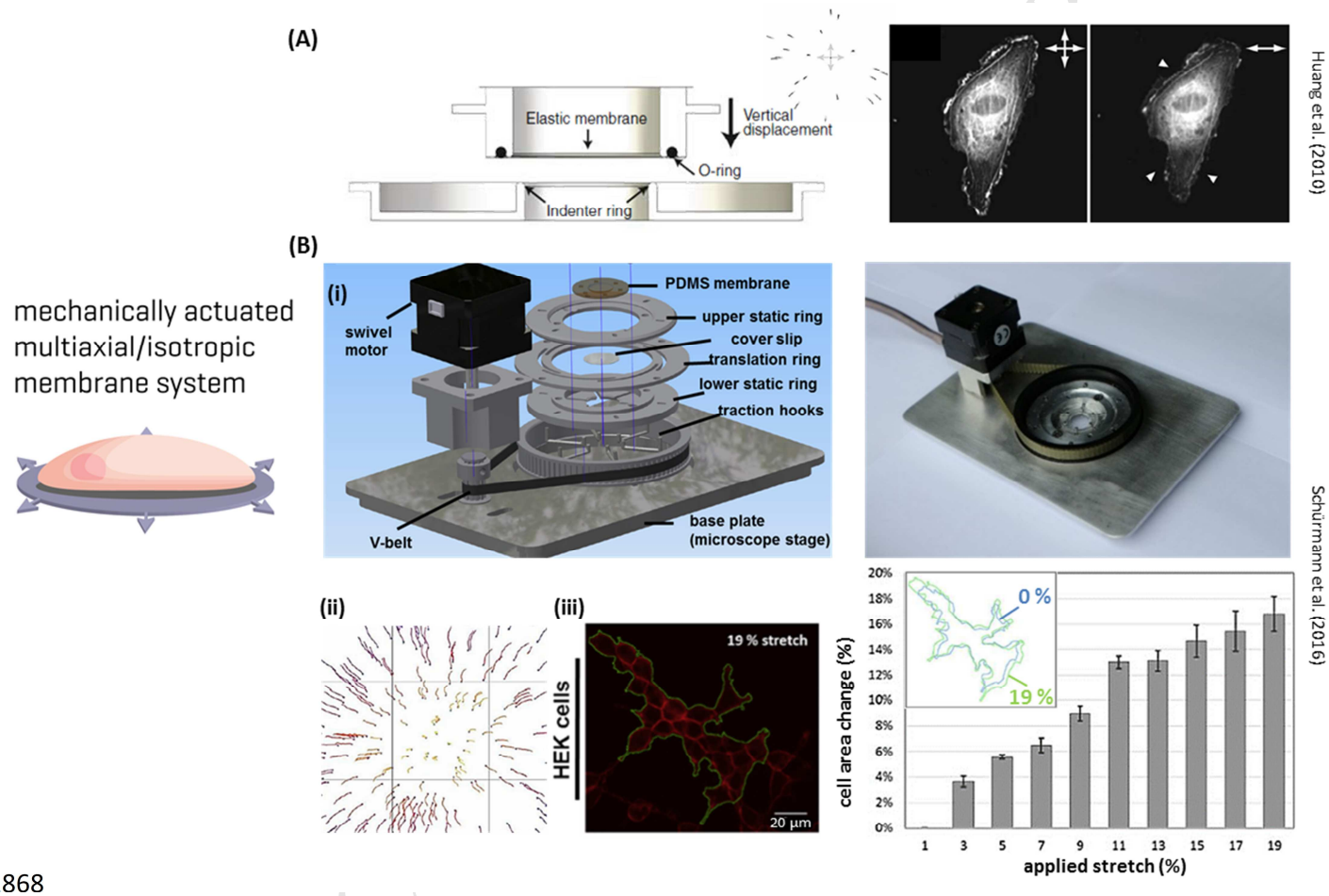

Figure 6 (Friedrich et al. 2017)

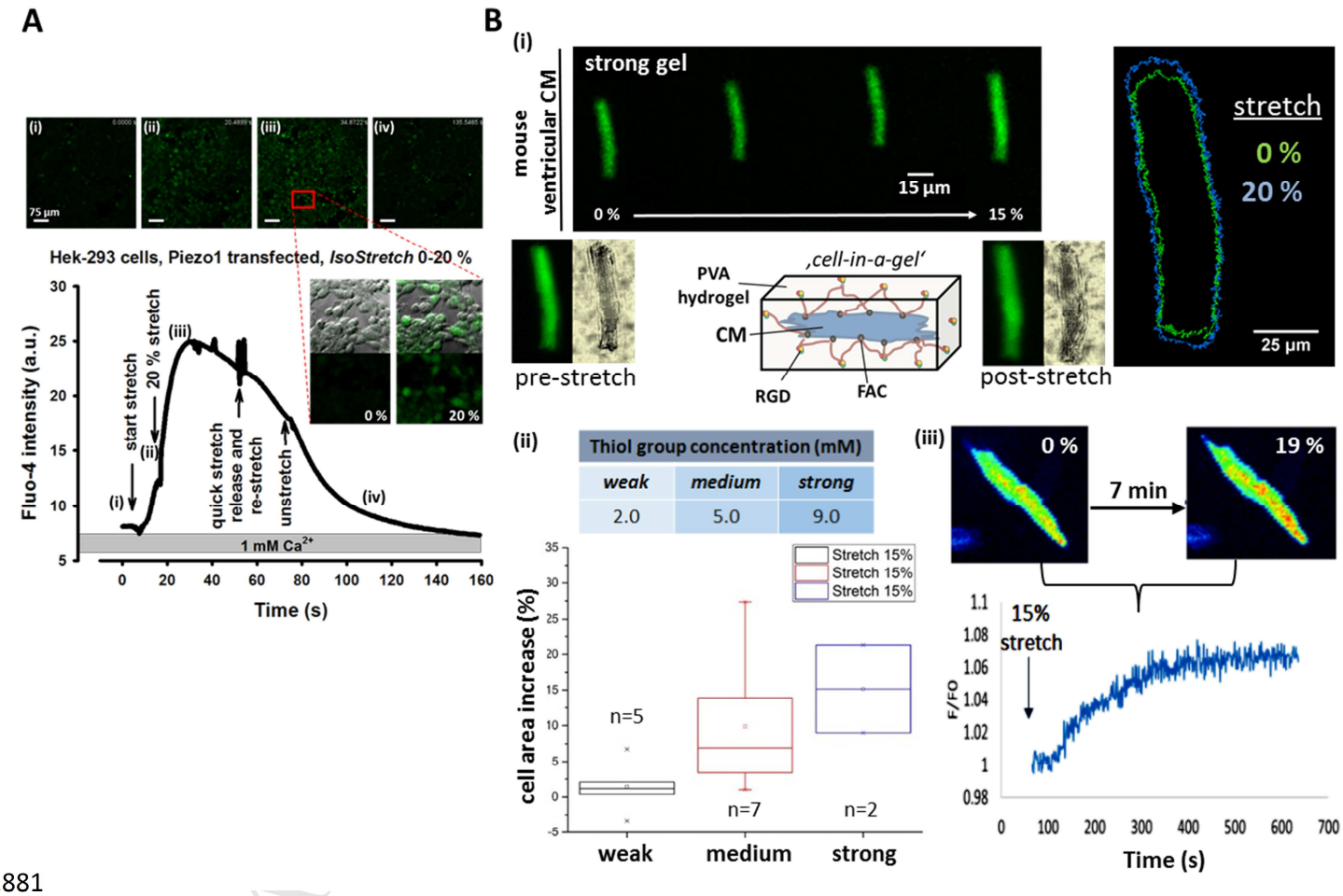

Figure 7 (Friedrich et al. 2017)